the eluate was collected in 1.9 ml fractions by an automatic fraction collector. Protein content and radioactivity of each fraction were measured by the Lowry-Folin method [23] and a well-type NaI-scintillation counter (ARC-300, Aloka, Tokyo, Japan), respectively.

Dialysis of Radiolabeled Tf

The solutions of DTPA-Tf and Tf incubated with ^{67}Ga or ^{111}In were poured into a dialysis bag (seamless cellulose tube, size:8/32 cm, Visking Company) and then dialyzed against 200 ml of PBS (pH 7.5). Radioactivity of the solution (2 µl) inside a dialysis bag was determined at 0, 2, 4, 8, and 24 h after dialysis.

Electrophoresis of Radiolabeled Tf

Duplicate 2 µl solution of DTPA-Tf and Tf incubated with ^{67}Ga or ^{111}In were applied to a cellulose acetate strip (2×6 cm). Electrophoresis was run at a constant current of 0.8 mA / cm in 0.069 M barbital buffer, pH 8.6, for 45 min. At the end of each run, one of the the duplicate strips was stained in Ponceau 3R for 2 min, destained in 1 % acetic acid, and aligned with the unstained strip to mark the location of Tf band. The Tf band on an unstained strip was cut out and the radioactivity was determined. The binding radioactivity to Tf was calculated as the percent of the total radioactivity applied on a strip.

Administration of ^{67}Ga, ^{111}In, ^{67}Ga-DTPA-Tf, and ^{111}In-DTPA-Tf

^{67}Ga or ^{111}In was diluted with saline to 185 kBq / ml. Each rat was intravenously injected with ^{67}Ga or ^{111}In in a dose of 37 kBq. In the case of ^{67}Ga –DTPA-Tf or ^{111}In-DTPA-Tf, two fractions corresponding to Tf eluted from G-50 columns to which radiolabeled DTPA-Tf was applied were combined and 200 µl of the solutions were intravenously injected into each rat.

Administration of $FeCl_3$

Each rat was intravenously injected with $FeCl_3$ (25 µmol / ml saline) at a dose of 100 µl 5 min before the administration of ^{67}Ga, ^{111}In, ^{67}Ga-DTPA-Tf, or ^{111}In-DTPA-Tf.

Determination of Blood Radioactivity

The rats injected with ^{67}Ga, ^{111}In, ^{67}Ga-DTPA-Tf, or ^{111}In-DTPA-Tf were anesthetized with urethane (1.5 g / kg, i.p.) 4 h after administration and the blood was obtained from the inferior vena cava. The radioactivity of the blood was determined by a well-type NaI-scintillation counter. The radioactivity ratios of ^{67}Ga or ^{111}In were expressed using the following formula:

Radioactivity ratio = A / B

A = sample activity (cpm) / sample weight (g)

B = total activity administered (cpm) / rat body weight (g)

RESULTS

Labeling Efficiency and Stability of Radiolabeled Tfs Using Gel Chromatography Method

Gel chromatography patterns of ^{67}Ga- or ^{67}Ga-DTPA-Tf and ^{111}In- or ^{111}In-DTPA-Tf are shown in (Figs. **1** and **2**), respectively. The labeling efficiencies of ^{67}Ga-Tf and ^{67}Ga-DTPA-Tf in pH 7.5 were 54 % and 100 %, respectively (Fig. **1-a, -c**). Low pH (pH 6.1) greatly affected the stability of ^{67}Ga-Tf and slightly affected the stability of ^{67}Ga-DTPA-Tf (Fig. **1-b, -d**). On the other hand, the labeling efficiencies of ^{111}In-Tf and ^{111}In-DTPA-Tf in pH 7.5 were both 100 % (Fig.

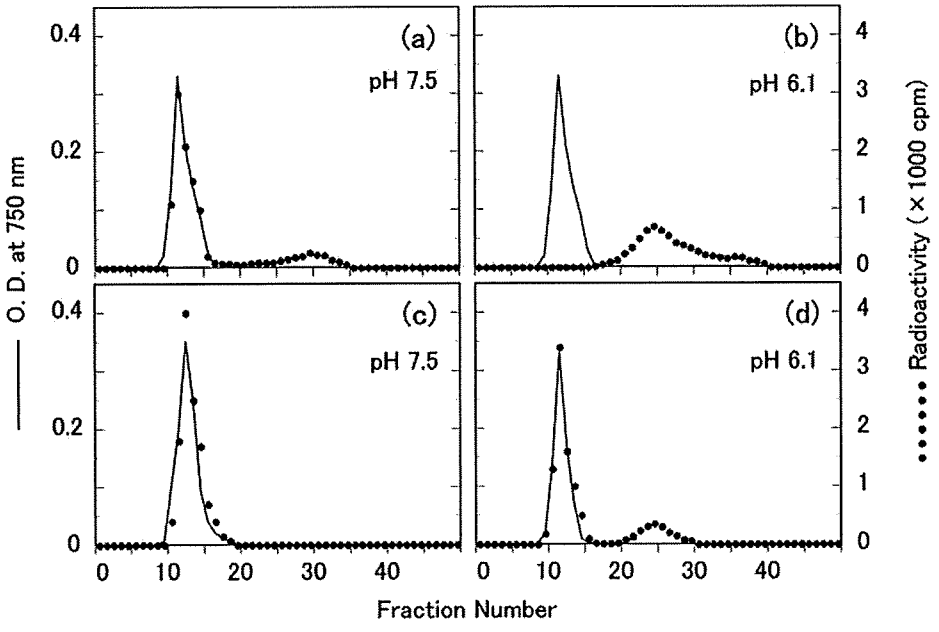

Figure 1. Labeling efficiencies and pH-stabilities of ^{67}Ga-Tf and ^{67}Ga-DTPA-Tf using Sephadex G-50 column chromatography. **(a)**: ^{67}Ga-Tf at pH 7.5, **(b)**: ^{67}Ga-Tf at pH6.1, **(c)**: ^{67}Ga-DTPA-Tf at pH7.5, **(d)**: ^{67}Ga-DTPA-Tf at pH6.1, solid line: protein, dot: radioactivity.

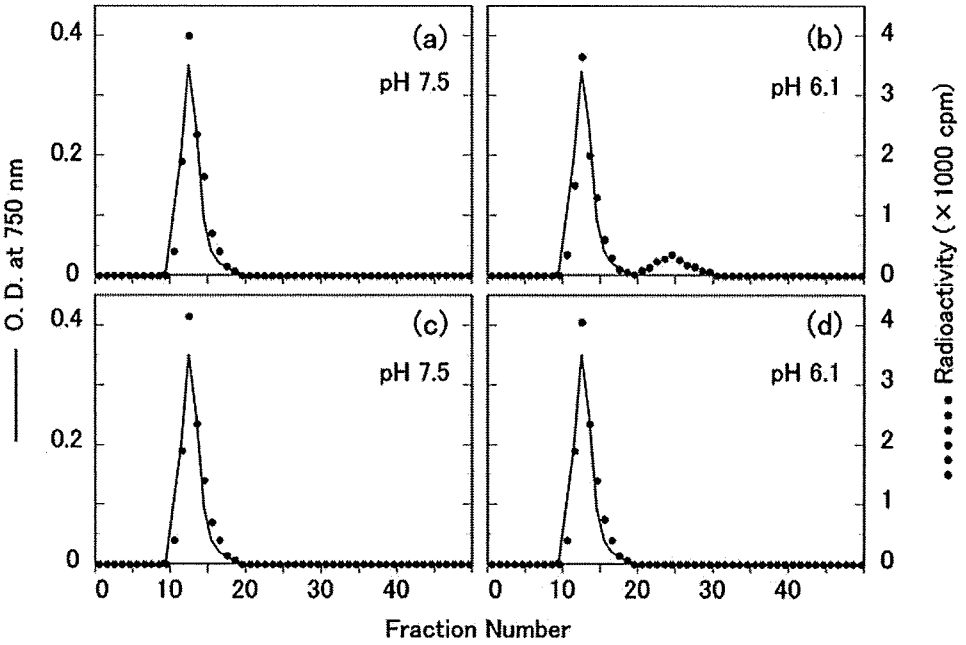

Figure 2. Labeling efficiencies and pH-stabilities of ^{111}In-Tf and ^{111}In-DTPA-Tf using Sephadex G-50 column chromatography. **(a)**: ^{111}In-Tf at pH7.5, **(b)**: ^{111}In-Tf at pH6.1, **(c)**: ^{111}In-DTPA-Tf at pH7.5, **(d)**: ^{111}In-DTPA-Tf at pH6.1, solid line: protein, dot: radioactivity.

2-a, -c). Low pH slightly affected the stability of ^{111}In-Tf but did not influence ^{111}In-DTPA-Tf stability at all (Fig. **2-b, -d**).

Stability of Radiolabeled Tfs Using Dialysis Method

The stabilities of ^{67}Ga-Tf or ^{67}Ga-DTPA-Tf and ^{111}In-Tf or ^{111}In-DTPA-Tf were studied by dialysis (Fig. **3**). Approximately 80 % of ^{67}Ga-Tf was dissociated 4 h after dialysis but ^{67}Ga-DTPA-Tf only underwent a low level of dissociation when measured 24 h after dialysis (Fig. **3-a**). On the other hand, there was no measurable dissociation of ^{111}In-Tf and ^{111}In-DTPA-Tf 24 h after dialysis (Fig. **3-b**).

Stability of Radiolabeled Tfs Using Electrophoresis Method

Binding percent of radioactivity to Tf or DTPA-Tf after electrophoresis is shown in Table **1**. In the case of ^{111}In-Tf and ^{111}In-DTPA-Tf, 66.3 % and 96.5 % of the radioactivity was bound to Tf, respectively, whereas only 25.7 % and 32.8 % in ^{67}Ga-Tf and ^{67}Ga-DTPA-Tf, respectively after electrophoresis.

Stability of Radiolabeled Tfs in the Blood

The stabilities of ^{67}Ga-Tf or ^{67}Ga-DTPA-Tf and ^{111}In-Tf or ^{111}In-DTPA-Tf in the blood are shown in (Fig. **4**). In order to inhibit ^{67}Ga or ^{111}In dissociated from Tf or DTPA-Tf from binding to Tf naturally existing in the blood, all of the Tf in the blood was saturated with Fe^{3+} by pre-injection of $FeCl_3$. The results showed that ^{67}Ga-Tf was the most unstable and ^{111}In-DTPA-Tf was the most stable among radiolabeled Tfs in the blood. Moreover, as the results demonstrated that pre-injection of $FeCl_3$ did not affect ^{111}In-DTPA-Tf but did influence ^{111}In-Tf, this might indicate that dissociated ^{111}In from ^{111}In-Tf bound Tf naturally existing in the blood without $FeCl_3$ and that ^{111}In did not dissociate from ^{111}In-DTPA-Tf at all.

DISCUSSION

The binding activity of ^{67}Ga to Tf is so weak that it undergoes dissociation during its passage through the column. On the contrary the binding activity of ^{111}In to Tf is stronger than that of ^{67}Ga. The results from dialysis and electrophoresis also showed that ^{111}In-Tf was more stable than ^{67}Ga-Tf. ^{67}Ga-DTPA-Tf and ^{111}In-DTPA-Tf were more stable than ^{67}Ga-Tf or ^{111}In-Tf in column chromatography and dialysis. ^{67}Ga-DTPA-Tf and ^{111}In-DTPA-Tf were more stable than ^{67}Ga-Tf or ^{111}In-Tf under low pH conditions. Vallabajosula *et al.* [24, 25] reported that acidic pH at the tumor site might be one of the factors involved in ^{67}Ga localization in tumors. Moreover, the reduction of pH below that of normal tissue

Table 1. Stabilities of ^{67}Ga-Tf, ^{67}Ga-DTPA-Tf, ^{111}In-Tf and ^{111}In-DTPA-Tf on Electrophoresis

	^{67}Ga-Tf	^{67}Ga-DTPA-Tf	^{111}In-Tf	^{111}In-DTPA-Tf
Binding percent (%)	25.7 ± 2.4#	32.8 ± 3.7#	66.3 ± 7.6#	96.5 ± 11.4#

#Data are expressed as the mean ± S.E. for 3 applications

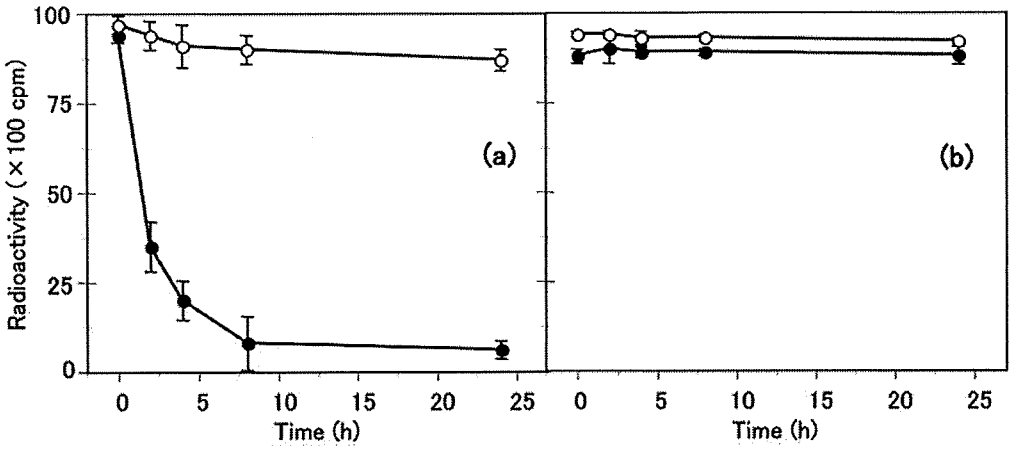

Figure 3. Stabilities of ^{67}Ga-Tf, ^{67}Ga-DTPA-Tf, ^{111}In-Tf and ^{111}In-DTPA-Tf on dialysis method. **(a)**: ^{67}Ga-Tf (•), ^{67}Ga -DTPA-Tf (○), **(b)**: ^{111}In-Tf (•), ^{111}In-DTPA-Tf (○).

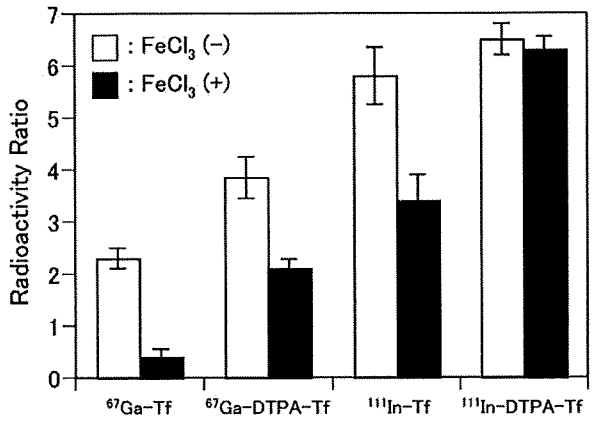

Figure 4. Stabilities of ^{67}Ga-Tf, ^{67}Ga-DTPA-Tf, ^{111}In-Tf and ^{111}In-DTPA-Tf in the blood.
Data are expressed as the mean ± S.E. for 4 rats.

(pH 7.4) might be due to the accumulation of lactic acid produced by anaerobic glycolysis. Additionally we think that acid glycosaminoglycans also reduce the pH at the site of granuloma or in tumor tissues. Therefore, the stability of radiolabeled Tf to low pH must be important for its uptake or accumulation into the target inflammatory tissues or tumors. The fact that ^{67}Ga- DTPA-Tf and ^{111}In-DTPA-Tf were more stable than ^{67}Ga-Tf or ^{111}In-Tf indicated that the binding of ^{67}Ga or ^{111}In to Tf via DTPA was stronger than the direct binding to Tf. However, ^{111}In-DTPA-Tf was more stable than ^{67}Ga-DTPA-Tf. This difference between the stabilities of ^{67}Ga-DTPA-Tf and ^{111}In-DTPA-Tf suggests that a part of ^{67}Ga and ^{111}In may directly bind to Tf at a binding site other than the DTPA conjugated site. ^{111}In-DTPA-Tf was the most stable *in vitro* among radiolabeled Tfs examined in the present study. In addition, we performed a preliminary study involved in stability of radiolabeled Tf *in vivo*. In the blood ^{111}In was not dissociated from DTPA-Tf at all, since preinjection of $FeCl_3$ did not affect the radioactivity ratio of ^{111}In-DTPA-Tf, whereas it did affect the radioactivity ratios of other radiolabeled Tfs. Fe^{3+} might also displace some ^{67}Ga or ^{111}In of ^{67}Ga-Tf, ^{67}Ga-DTPA-Tf, or ^{111}In-Tf. The dissociated ^{67}Ga or ^{111}In is excreted into urine [4, 6] and the radioactivity ratios in the blood must decrease. ^{111}In-DTPA-Tf was the most stable *in vitro* and *in vivo* among radiolabeled Tfs examined in the present study.

DTPA-Tf can be stored for a long time and is easily radiolabeled with ^{111}In on demand. From the results of the present study, it is clear that ^{111}In-DTPA-Tf is a readily available and useful tool for the experimental study of the physiological roles of Tf and Tf receptors. Moreover if Tf is used as a drug delivery agent, ^{111}In-DTPA-Tf would be a valuable tool for the confirmation of the site to which drug is delivered.

REFERENCES

[1] Ohkubo, Y., Shibuya, A., Kohno, H. and Kubodera, A. Involvement of transferrin in the uptake of 67Ga in inflammatory and normal tissues. (1989) *Int. J. Rad. Appl. Instrum. B, 16*, 337.

[2] Ohkubo, Y., Sawamura, H., Katoh, S., Sasayama, A., Abe, K., Kohno, H. and Kubodera, A. Studies on 67Ga uptake by mouse granuloma tissues. (1991) *Int. J. Rad. Appl. Instrum. B, 18*, 205.

[3] Ohkubo, Y., Sasayama, A., Takegahara, I., Katoh, S., Abe, K., Kohno, H. and Kubodera, A. 67Ga in transferrin-unbound form is taken up by inflamed liver of mouse treated with CCl4. (1990) *Ann. Nucl. Med., 4*, 89.

[4] Abe, S., Hasegawa, S., Nirasawa, M., Sato, N. and Ohkubo, Y. Free 67Ga enters into the hepatocytes of carbon tetrachloride-treated rats. (2003) *Hepatol. Res., 25*, 306.

[5] Ohkubo, Y., Araki, S., Abe, K., Takasu, S., Kohno, H. and Kubodera, A. The effect of FeCl3 on the accumulation of gallium-67 into inflammatory and normal tissues. (1988) *Ann. Nucl. Med., 2*, 59.

[6] Abe, S., Hasegawa, S., Nirasawa, M., Sasaki, M. and Ohkubo, Y. Transferrin is not involved in the entry of 67Ga into hepatocytes from regenerating liver of partially hepatectomized rats. (2001) *Biol. Pharm. Bull., 24*, 1343.

[7] Sato, R., Abe, S., Yamada, Y., Toyama, D., Ohtake, Y., Sato, N. and Ohkubo, Y. The entering of indium-111 and iron-59 into the hepatocytes from partially hepatectomized rats differ from that of gallium-67. (2004) *Biol. Pharm. Bull., 27*, 1193.

[8] Ohkubo, Y., Abe, K., Kohno, H., Katoh, S. and Kubodera, A. 111In (III) uptake by inflammatory and normal tissues. (1989) *Ann. Nucl. Med., 3*, 135.

[9] Salter-Cid, L., Brunmark, A., Li, Y., Leturcq, D., Peterson, P. A., Jackson, M. R. and Yang, Y. Transferrin receptor is negatively modulated by the hemochromatosis protein HFE: implications for

cellular iron homeostasis. (1999) *Proc. Natl. Acad. Sci. USA*, *96*, 5434.

[10] Roetto, A., Daraio, F., Alberti, F., Porporato, P., Cali, A., De Gobbi, M. and Camaschella, C. Hemochromatosis due to mutations in transferrin receptor 2. (2002) *Blood Cells Mol. Dis.*, *29*, 465.

[11] Fleming, R. E., Ahmann, J. R., Migas, M. C., Waheed, A., Koeffler, H. P., Kawabata, H., Britton, R. S., Bacon, B. R. and Sly, W. S. Targeted mutagenesis of the murine transferrin receptor-2 gene produces hemochromatosis. (2002) *Proc. Natl. Acad. Sci. USA*, *99*, 10653.

[12] Drake, S. F., Morgan, E. H., Herbison, C. E., Delima, R., Graham, R. M., Chua, A. C., Leedman, P. J., Fleming, R. E., Bacon, B. R., Olynyk, J. K. and Trinder, D. Iron absorption and hepatic iron uptake are increased in a transferrin receptor 2 (Y245X) mutant mouse model of hemochromatosis type 3. (2007) *Am. J. Physiol. Gastrointest. Liver Physiol.*, *292*, G323.

[13] Kawabata, H., Germain, R. S., Vuong, P. T., Nakamaki, T., Said, J. W. and Koeffler, H. P. Transferrin receptor 2-alpha supports cell growth both in iron-chelated cultured cells and *in vivo*. (2000) *J. Biol. Chem.*, *275*, 16618.

[14] Lee, A. W., Oates, P. S. and Trinder, D. Effects of cell proliferation on the uptake of transferrin-bound iron by human hepatoma cells. (2003) *Hepatology*, *38*, 967-77.

[15] Radoshitzky, S. R., Abraham, J., Spiropoulou, C. F., Kuhn, J. H., Nguyen, D., Li, W., Nagel, J., Schmidt, P. J., Nunberg, J. H. andrews, N. C., Farzan, M. and Choe, H. Transferrin receptor 1 is a cellular receptor for New World haemorrhagic fever arenaviruses. (2007) *Nature*, *446*, 92.

[16] Raje, C. I., Kumar, S., Harle, A., Nanda, J. S. and Raje, M. The macrophage cell surface glyceraldehyde-3-phosphate dehydrogenase is a novel transferrin receptor. (2007) *J. Biol. Chem.*, *282*, 3252.

[17] Qian, Z. M., Li, H., Sun, H. and Ho, K. Targeted drug delivery via the transferrin receptor-mediated endocytosis pathway. (2002) *Pharmacol. Rev.*, *54*, 561.

[18] Kojima, S. and Jay, M. Comparisons of labeling efficiency, biological activity and biodistribution among 125I-, 67Ga-DTPA-and 67Ga-DFO-lectins. (1987) *Eur. J. Nucl. Med.*, *13*, 366.

[19] Arano, Y., Mukai, T., Akizawa, H., Uezono, T., Motonari, H., Wakisaka, K., Kairiyama, C. and Yokoyama, A. Radiolabeled metabolites of proteins play a critical role in radioactivity elimination from the liver. (1995) *Nucl. Med. Biol.*, *22*, 555.

[20] Hnatowich, D. J., Griffin, T. W., Kosciuczyk, C., Rusckowski, M., Childs, R. L., Mattis, J. A., Shealy, D. and Doherty, P. W. Pharmacokinetics of an indium-111-labeled monoclonal antibody in cancer patients. (1985) *J. Nucl. Med.*, *26*, 849.

[21] Gangopadhyay, A., Petrick, A. T. and Thomas, P. Modification of antibody isoelectric point affects biodistribution of 111-indium-labeled antibody. (1996) *Nucl. Med. Biol.*, *23*, 257-61.

[22] Krejcarek, G. E. and Tucker, K. L. Covalent attachment of chelating groups to macromolecules. (1977) *Biochem. Biophys. Res. Commun.*, *77*, 581.

[23] Lowry, O. H., Rosebrough, N. J., Farr, A. L. and Randall, R. J. Protein measurement with the Folin phenol reagent. (1951) *J. Biol. Chem.*, *193*, 265.

[24] Vallabhajosula, S. R., Harwig, J. F. and Wolf, W. The mechanism of tumor localization of gallium-67 citrate: role of transferrin binding and effect of tumor pH. (1981) *Int. J. Nucl. Med. Biol.*, *8*, 363.

[25] Vallabhajosula, S. R., Harwig, J. F. and Wolf, W. Effect of pH on tumor cell uptake of radiogallium *in vitro* and *in vivo*. (1982) *Eur. J. Nucl. Med.*, *7*, 462.

Received: July 27, 2008 **Revised: August 13, 2008** **Accepted: August 19, 2008**

ELSEVIER

Journal of Hepatology 48 (2008) 246–254

Journal of Hepatology

www.elsevier.com/locate/jhep

Effect of aging on EGF-induced proliferative response in primary cultured periportal and perivenous hepatocytes☆

Yosuke Ohtake[1,*], Akiko Maruko[1], Nao Ohishi[1], Manabu Fukumoto[2], Yasuhito Ohkubo[1]

[1]*Department of Radiopharmacy, Tohoku Pharmaceutical University, 4-4-1, Komatsushima, Aoba-ku, Sendai, Miyagi 981-8558, Japan*
[2]*Department of Pathology, Institute of Development, Aging and Cancer, Tohoku University, 4-1, Seiryo-machi, Aoba-ku, Sendai, Miyagi 980-8575, Japan*

***Background/Aims*: Aging relates to declined proliferative capacity of the liver, but the molecular mechanism is not well understood. We examined whether functional changes of epidermal growth factor (EGF) receptor (EGFR) are involved in age-related decline in EGF-induced DNA synthesis using hepatocytes isolated in periportal and perivenous regions of the liver, which differ in the proliferative capacity.**

***Methods*: Periportal hepatocytes (PPH) and perivenous hepatocytes (PVH) in 7-, 30-, and 90-week-old rats were isolated using the digitonin/collagenase perfusion technique. DNA synthesis was assessed by [methyl-^{3}H]thymidine incorporation. EGFR binding affinity to EGF was analyzed by Scatchard analysis using [^{125}I]EGF. EGFR dimerization and phosphorylation were determined by Western blot analysis.**

***Results*: EGF-induced DNA synthesis was greater in PPH than in PVH from rats of 7 weeks, but the zonal difference disappeared with aging. [^{125}I]EGF binding studies indicated that high-affinity EGFR in both subpopulations also disappeared with aging. Furthermore, EGF-induced dimerization in both subpopulations was down-regulated with aging, and the pattern of EGFR phosphorylation was parallel to that of dimerization.**

***Conclusions*: These data suggest that age-related decline in EGF-induced DNA synthesis of PPH and PVH is caused by down-regulation of EGFR dimerization through the decrease of high-affinity EGFR.**

Keywords: **Aging; DNA synthesis; EGF; EGFR; Periportal hepatocytes; Perivenous hepatocytes**

1. Introduction

A decline in proliferative capacity is an important hallmark of mammalian aging in many cell types. Hepatocytes have proven to be a particularly good model to study the mechanisms associated with this phenomenon. Liver regeneration is impaired in aged animals as evidenced by a delay and reduction in magnitude of DNA synthesis [1,2]. Epidermal growth factor (EGF)-stimulated DNA synthesis is markedly lower in primary cultured hepatocytes from aged rats compared to similarly treated cells of young rats [3].

EGF is well recognized as a potent mitogen [4]. Transmembrane signaling events occur when EGF binds to cell surface receptor, and a subclass of high-affinity EGF receptor (EGFR) contributes to activation of the EGFR signal transduction cascade [5,6]. Binding of EGF to the receptor causes the dimerization between EGFRs and induces the phosphorylation of tyrosine residues on the receptor and thereafter leads to activation of extracellular signal-regulated kinase (ERK),

Received 25 March 2007; received in revised form 17 July 2007; accepted 20 August 2007; available online 15 October 2007
Associate Editor: C. Trautwein

☆ The authors declare that they do not have anything to disclose regarding funding or conflict of interest with respect to this manuscript.

* Corresponding author. Tel.: +81 22 727 0121; fax: +81 22 275 2013.
E-mail address: y-ohtake@tohoku-pharm.ac.jp (Y. Ohtake).

0168-8278/$32.00
doi:10.1016/j.jhep.2007.08.009

resulting in the induction of cell growth [4]. Others have demonstrated that age-related decline in DNA synthesis of cultured hepatocytes reflects a decline in the activation of ERK, which plays a critical role in transmitting proliferative signals to the nucleus [3]. Neither EGFR number nor affinity of the receptor for its ligand alters with aging [3]. On the other hand, an early study indicated that the number and affinity of EGFRs were changed in aged rats [7]. The change with aging is not consistent with other findings and is controversial, and no mechanism has ever been proposed for this observation. The molecular mechanism underlying the age-related decline in proliferative response is not well understood.

Hepatocytes in liver parenchyma are classified as periportal hepatocytes (PPH) and perivenous hepatocytes (PVH) according to studies showing zonal differences in metabolism [8,9] and proliferation [10–13]. In regenerating rat liver after partial hepatectomy, PPH and PVH show differential growth capacities, and DNA synthesis in PPH is greater than in PVH [11,12]. In a cultured system, PPH and PVH show different responses to EGF due, at least in part, to the heterogeneous distribution of EGFR [13,14].

These findings raise the possibility that a potential explanation for age-related decline in proliferative response may be obtained by taking account for a zonal difference in EGFR number and affinity in a primary cultured system.

In the present study, we investigated the age-related differences in the characteristics of EGFR including number and affinity for its ligand, dimerization and phosphorylation in primary cultured PPH and PVH obtained from 7-, 30-, and 90-week-old rats.

2. Materials and methods

2.1. Animals and materials

Male 7-, 30-, and 90-week-old Wistar rats (SLC, Hamamatsu, Japan) were kept at a controlled temperature (23 ± 1 °C) under a 12 h light–dark cycle and were maintained with a standard diet and water. All animal experiments were performed in strict accordance with our institutional Animal Committee's criteria for the care and use of laboratory animals. [Methyl-^{3}H]thymidine and [^{125}I]EGF were from Perkin-Elmer Life Sciences, Inc. (Boston, MA). Collagenase was from Nitta Gelatin (Osaka, Japan). Digitonin was from Sigma–Aldrich (St. Louis, MO). Mouse EGF was from Biomedical Technologies, Inc. (Stoughton, MA, USA). Anti-ErbB-1 (EGFR) polyclonal antibody and anti-phospho-EGFR at Y1173 antibody were from Santa Cruz Biotechnology Inc. (Santa Cruz, CA).

2.2. Isolation and culture of whole hepatocytes, PPH and PVH

Whole hepatocytes were isolated by collagenase perfusion. PPH and PVH were isolated from separate animals using the digitonin/collagenase perfusion and the detailed procedure has been described previously [11]. Viability of hepatocytes was determined by trypan blue staining and was at a level of more than 90%. PPH and PVH were placed in 12-well collagen-coated plates (Iwaki, Tokyo, Japan) at a density of 0.8×10^5 cells/cm^2 in Williams' E (WE) medium containing 10% fetal bovine serum, 10^{-9} M insulin, 10^{-9} M dexamethasone, 1% (v/v) antibiotics (GIBCO, Grand Island, NY). After 3 h incubation, the medium was replaced with serum-free medium.

2.3. Confirmation of separation of PPH and PVH

Separation of PPH and PVH was confirmed by measuring enrichment in two specific marker enzymes, alanine aminotransferase (ALT) for PPH [15] and glutamine synthetase (GS) for PVH [16].

2.4. Measurement of DNA synthesis

DNA synthesis was measured with or without 10^{-8} M EGF, a concentration which induced the maximum proliferative effect and was assessed by [methyl-^{3}H]thymidine incorporation into hepatocytes. The radioactivity of [methyl-^{3}H]thymidine incorporated into cells was measured using a Beckman LS 6500 liquid scintillation counter (Beckman Coulter, Fullerton, CA, USA).

2.5. Assay for binding of [^{125}I]EGF to cultured hepatocytes

The assay for binding of ligand containing 10 pM [^{125}I]EGF (specific activity; 81.4 TBq/mmol) and various concentrations of unlabeled EGF to cultured hepatocytes was performed as described previously [13]. Radioactivity of [^{125}I]EGF bound to hepatocytes was measured using a gamma counter (Aloca ARC-370M, Tokyo, Japan).

2.6. Cross-linking of EGFRs

After treatment with EGF for indicated times, the hepatocytes were incubated for 1 h at 4 °C with 2 mM bis-(sulfosuccinimidyl) suberate (BS^3) (Pierce), cross-linking reagent. The quench solution (0.5 M Tris–HCl buffer, pH 7.4) was then added to a final concentration of 0.25 M and incubated for 10 min at 4 °C. The hepatocytes were subjected to hepatic membrane fractionation.

2.7. Hepatic membrane fractionation

Cultured hepatocytes were homogenized in 50 mM Tris–HCl buffer containing 1 mM EDTA, and 10% glycerol supplemented with 1% protease inhibitor cocktail (Sigma–Aldrich) with 30 strokes on a Dounce homogenizer. The homogenates were then centrifuged at 500g for 5 min. The supernatant was collected and centrifuged at 100,000g for 30 min. The pellet containing hepatic membranes was subjected to Western blotting analysis.

2.8. Western blotting analysis

The hepatic membranes were mixed with sample buffer for sodium dodecyl sulfate (SDS)–polyacrylamide gel electrophoresis containing 62.5 mM Tris–HCl buffer (pH 6.8), 10% glycerol, 2% SDS, 5% β-mercaptoethanol, and 0.025% bromophenol blue. The mixture was boiled at 100 °C for 3 min and was size separated by SDS–polyacrylamide gel electrophoresis on 3–10% polyacrylamide gradient gel (Bio-Rad). The separated membrane proteins were transferred onto polyvinylidene difluoride (PVDF) membranes (GE healthcare) and immunoblot analysis was carried out using the appropriate antibodies. Immunoreactive bands were detected with ECL Western blotting detection reagents (GE healthcare) and exposed with X-ray film (FUJIFILM).

2.9. Statistical analysis

The Mann–Whitney test was used for the statistical analysis of [methyl-^{3}H]thymidine incorporation in PPH and PVH. For the binding assay of [^{125}I]EGF, K_d values of PPH and PVH were compared as correlation coefficients.

3. Results

3.1. Isolation of PPH and PVH

PPH and PVH, isolated by the digitonin/collagenase perfusion technique, from rats of various ages were identified by measuring the activities of specific marker enzymes (ALT and GS) (Table 1). The activities of ALT and GS in PPH and PVH were consistent with previous reports [13], and in good agreement with published values [17,18], showing a successful isolation of PPH and PVH.

3.2. Effect of aging on EGF-induced DNA synthesis in primary cultured whole hepatocytes, PPH and PVH

We investigated DNA synthesis induced by EGF treatment in primary cultured whole hepatocytes, PPH and PVH from rats of various ages (Fig. 1). EGF-induced DNA synthesis in whole hepatocytes gradually decreased with aging, and in 90-week-old rats, did not differ from control levels (Fig. 1a–c; left graph). In 7-week-old rats, EGF-induced DNA synthesis in PPH gradually increased to 3 times the control level at 72 h. In PVH, EGF increased DNA synthesis to twice the

Table 1
Effect of aging on enzymatic characteristics in primary cultured PPH and PVH obtained from 7-, 30-, and 90-week-old rats

Marker enzyme	Age	Times after primary culture (h)	PPH specific activity[c]	PVH specific activity[c]	PVH/PPH ratio
ALT[a]	7 weeks	24	448 ± 53	221 ± 41	0.49
		48	391 ± 46	209 ± 27	0.53
		72	315 ± 31	185 ± 18	0.58
	30 weeks	24	401 ± 39	198 ± 21	0.49
		48	358 ± 48	201 ± 30	0.56
		72	299 ± 25	179 ± 28	0.49
	90 weeks	24	423 ± 63	203 ± 15	0.48
		48	360 ± 33	183 ± 24	0.51
		72	305 ± 30	165 ± 27	0.54
GS[b]	7 weeks	24	82 ± 19	1023 ± 157	12
		48	76 ± 22	956 ± 178	13
		72	72 ± 17	711 ± 118	10
	30 weeks	24	74 ± 13	875 ± 201	12
		48	70 ± 9	732 ± 102	10
		72	60 ± 17	685 ± 89	11
	90 weeks	24	62 ± 8	513 ± 79	8
		48	56 ± 11	439 ± 55	8
		72	53 ± 14	402 ± 28	7

Note. Hepatocytes were plated at cell density of 0.8×10 cells/cm^2. Hepatocytes obtained from each aged rats were cultured in the presence of EGF for 24, 48, and 72 h. Each specific marker were measured as described in Section 2.

[a] Specific activity of ALT was expressed as IU/mg protein.

[b] Specific activity of GS was expressed as mU/mg protein.

[c] All activities represent means ± SEM of 3–4 experiments.

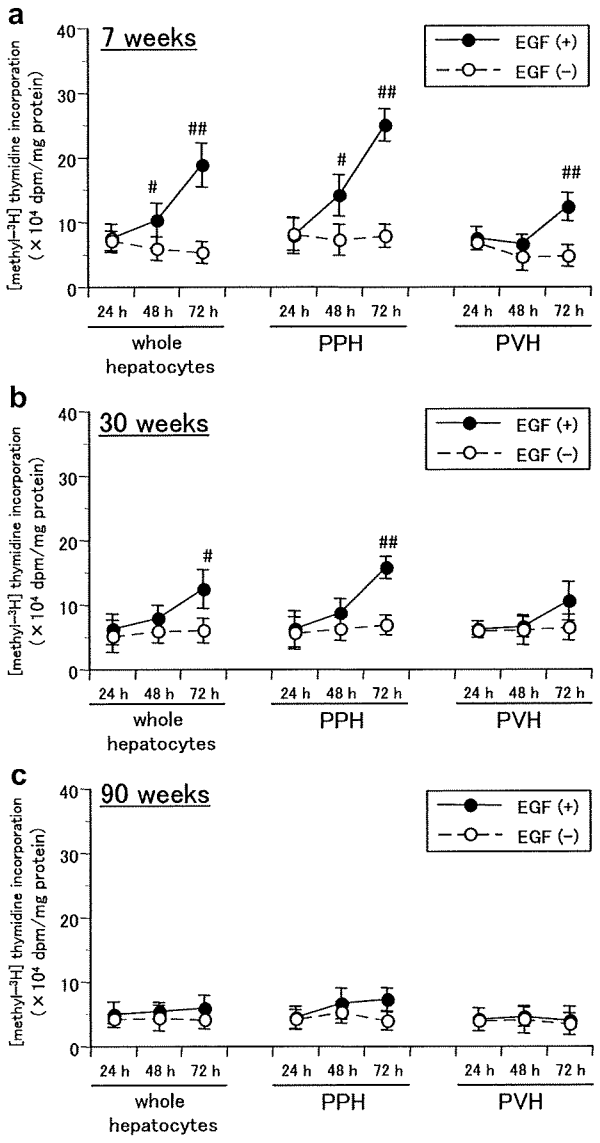

Fig. 1. Effect of aging on DNA synthesis in primary cultured whole hepatocytes, PPH and PVH obtained from (a) 7-, (b) 30-, and (c) 90-week-old rats. DNA synthesis induced by EGF (10^{-8} M) treatment was measured by the [methyl-^{3}H]thymidine incorporation method as described in Section 2. [Methyl-^{3}H]thymidine was included from 0 to 24 h, 24 to 48 h, and 48 to 72 h. The addition of 10 ng/ml of aphidicolin, which is a specific inhibitor of the replicative enzyme, DNA polymerase α, to cultured hepatocytes obtained from rats of various ages completely abolished EGF stimulated [methyl-^{3}H]thymidine incorporation without any effect on cell viability (data not shown). Each value represents the mean ± SEM of 3–4 samples. $^{\#}P < 0.05$, $^{\#\#}P < 0.01$, versus respective EGF-untreated group.

control level at 72 h. The effect of EGF on DNA synthesis was greater in PPH than in PVH (Fig. 1a). In 30-week-old rats, DNA synthesis 72 h after EGF treatment in PPH was reduced to about 70% of the level in 7-week-old rats (Fig. 1b). EGF-induced DNA synthesis in PVH was also reduced compared with 7-week-old rats and did not differ from the control levels (Fig. 1b). In 90-week-old rats, EGF-induced DNA syntheses in both subpopulations significantly decreased and did not differ from the control levels (Fig. 1c). DNA synthesis in whole hepatocytes obtained from 7-, 30-, and 90-week-old rats showed their intermediate value between PPH and PVH.

3.3. Effect of aging on EGF binding to primary cultured PPH and PVH

Next, we investigated [^{125}I]EGF binding to hepatocytes from rats of various ages. Fig. 2 shows a Scatchard plot of bound/free [^{125}I]EGF and the [^{125}I]EGF binding rate to the receptor. Fig. 2 (insets) shows saturation curves of [^{125}I]EGF-specific binding to its receptor. As shown in Fig. 2a, a Scatchard plot of the binding data in PPH from 7-week-old rats was curvilinear and yielded two apparent dissociation constants (K_d) of 9.01 pM (high-affinity) and 127 pM (low-affinity). The number of binding sites (B_{max}) was 0.92 (high-affinity) and 6.69 (low-affinity) pM, respectively. In PVH from 7-week-old rats, K_d values were 25.7 (high-affinity) and 239 (low-affinity) pM, and B_{max} values were 1.40 (high-affinity) and 7.47 (low-affinity) pM, respectively. PPH was found to have a greater affinity than PVH for EGF, whereas there was no significant difference in B_{max} values between PPH and PVH. In 30-week-old rats, K_d values in PPH were 22.8 (high-affinity) and 128 (low-affinity) pM, and B_{max} values were 1.75 (high-affinity) and 6.04 (low-affinity) pM, respectively (Fig. 2b). On the other hand, in PVH from 30-week-old rats, K_d value was 192 (low-affinity) pM, and B_{max} value was 5.90 (low-affinity) pM (Fig. 2b). The high-affinity EGFRs in both subpopulations from 30-week-old rats were down-regulated and that in PVH completely disappeared. In 90-week-old rats, the K_d value for the low-affinity EGFR in PPH was 147 pM, and B_{max} was 5.44 pM (Fig. 2c). In PVH, the K_d value was 196 pM, and B_{max} was 5.15 pM (Fig. 2c). The high-affinity EGFR was down-regulated and completely disappeared in both cell subpopulations.

3.4. Effect of aging on EGFR dimerization in primary cultured PPH and PVH

Next, we investigated the effect of aging on EGFR dimerization. The addition of EGF-induced redistribution of the receptor from the 170–175 kDa band to the 340–350 kDa band corresponding to the monomeric and dimeric forms of the EGFR, respectively. As the

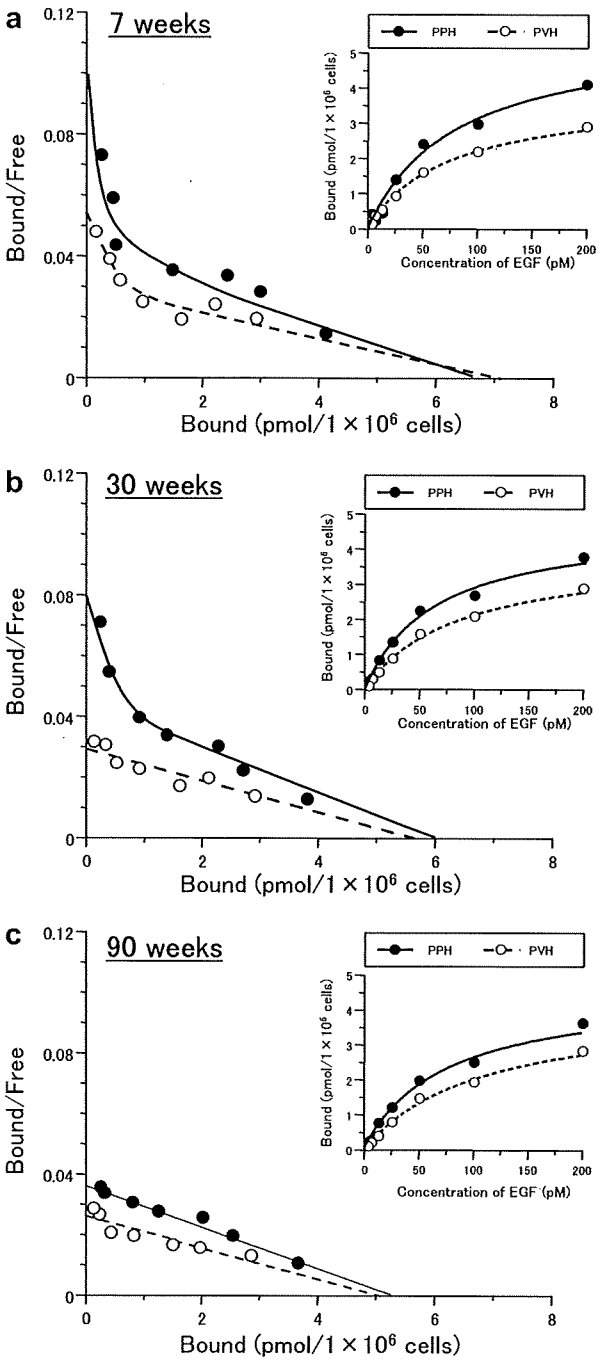

Fig. 2. Scatchard analysis of EGF binding to primary cultured PPH and PVH obtained from (a) 7-, (b) 30-, and (c) 90-week-old rats. Ligand binding affinities were determined at a fixed concentration of ^{125}I-EGF by competition with unlabeled EGF (see Section 2). All points were done in duplicate and experiments were repeated a minimum of three times. Scatchard plots and estimates of ligand binding affinities and receptor numbers were analyzed using GraphPad Prism 5.00. The inset panel shows saturation curves of [^{125}I]EGF-specific binding to its receptor.

control for EGFR activation, hepatic membranes from cultured hepatocytes without EGF treatment were used (Fig. 3a, lane 1). As shown in Fig. 3, the dimerization of

EGFRs in PPH and PVH from 7-week-old rats greatly increased in response to EGF stimulation. The maximum dimerization was achieved within 5 min following EGF treatment and was sustained at this level for 30 min post-treatment and thereafter decreased. The dimerization of EGFRs following EGF treatment was greater in PPH than in PVH obtained from 7-week-old rats. By comparison, in 30-week-old rats EGF stimulation of each subpopulation resulted in less dimerization of EGFRs than in 7-week-old rats, although the temporal patterns in dimerization in each subpopulation from 30-week-old were not different compared to 7-week-old rats. In 90-week-old rats, the dimerization of EGFRs in each subpopulation significantly decreased in response to EGF stimulation, and the rate of dimerization was not different between PPH and PVH.

3.5. Effect of aging on EGFR phosphorylation in primary cultured PPH and PVH

We have studied the effect of aging on activation of EGFR following EGF treatment by Western blot analysis with antibodies, which specially recognize EGFR phosphorylated at Y1173. As the control for EGFR activation, hepatic membranes from cultured hepatocytes without EGF treatment were used (Fig. 4a, lane 1). As shown in Fig. 4, the phosphorylation of EGFR on hepatic membranes from rats of various ages resulted in good correlations with its dimerization. In 90-week-old rats, the phosphorylation of EGFR was almost undetected in both subpopulations.

4. Discussion

Numerous studies using various models have provided evidence that aging is associated with a decline in proliferative response [3,19–22]. However, the molecular basis of this age-related decline in proliferative response is not well understood. To understand this phenomenon in detail, we examined hepatocytes isolated in periportal and perivenous regions of the liver, which differ in proliferative capacity [11,13,23,24]. EGF-induced DNA synthesis in both subpopulations decreased with aging, and in 90-week-old rats the difference in DNA synthesis between PPH and PVH completely disappeared (Fig. 1). We and others reported that PPH responded to EGF with higher sensitivity than PVH [13,23,24]. However, the present data indicated that zonal differences in EGF-induced DNA synthesis in both subpopulations were abolished with aging. At this point, there is one potential problem that PPH and PVH may be not sufficiently isolated by the digitonin/collagenase perfusion technique because the exposure to digitonin may differ in the size of the liver with age of the rats. To overcome this, we provided data on the response of EGF to whole hepatocytes, mixture of PPH and PVH, isolated in a standard collagenase perfusion (Fig. 1). As a result, DNA synthesis in whole hepatocytes decreased with aging and showed the intermediate value between PPH and PVH. Therefore, the reason for a drastic change of DNA synthesis in both subpopulations with aging is that the characteristics of EGFR must be changed with aging.

In Scatchard analysis (Fig. 2), EGFR on PPH responded to EGF with higher sensitivity than that on PVH in 7-week-old rats. However, in 30-week-old rats, a subclass of high-affinity EGFR on PVH disappeared, and in 90-week-old rats, high-affinity EGFR on PPH also disappeared. On the other hand, in a subclass of low-affinity EGFR on PPH and PVH, there was no significant difference in K_d and B_{max} values with aging. These results suggest that a subclass of high- but not low-affinity EGFR is down-regulated with aging. Others demonstrated that the activation of the EGFR signal transduction cascade could occur completely through exclusive binding of EGF to a subclass of high-affinity EGFR [5,6]. Moreover, we indicated that differential growth capacities of PPH and PVH were involved in the relative amount of a subclass of high-affinity EGFR [13]. Considering the results of previous reports in addition to the present one, it is possible that down-regulation of a subclass of high-affinity EGFR with aging causes age-related decline in DNA synthesis of primary cultured hepatocytes in both subpopulations.

Ishigami et al. reported that EGF-induced DNA synthesis in cultured rat hepatocytes reduced with aging, and this reduction was not due to decreased receptor density or specific binding affinity [3]. However, in our EGF binding study, there was an age-related decline of binding affinity of EGFR (Fig. 2). Moreover, Marti indicated that in isolated hepatic membranes from 7- and 90-week-old rats, EGFR number and affinity for its ligand significantly decreased with aging [7]. A possible reason for the discrepancy is the different conditions used for primary culture, *e.g.*, hepatocytes are cultured at low density in the examination system used by Ishigami et al. Hepatocyte-proliferation and liver-specific differentiation functions are known to be reciprocally regulated by the cell density in culture [25–27]. It has been reported that when hepatocytes are grown at low density, they undergo a rapid loss of liver-specific functions [28]. Indeed, the previous results showed that specific markers in each population were abolished in cells cultured at low density [13]. Another possible reason is that the zonal differences between PPH and PVH are not considered. In the present study, we demonstrated that when PPH and PVH from rats of various ages were cultured at high density, zonal characteristics in both subpopulations were sustained (Table 1). Therefore, we think that high density primary culture of hepatocytes provides a good model for studying their charac-

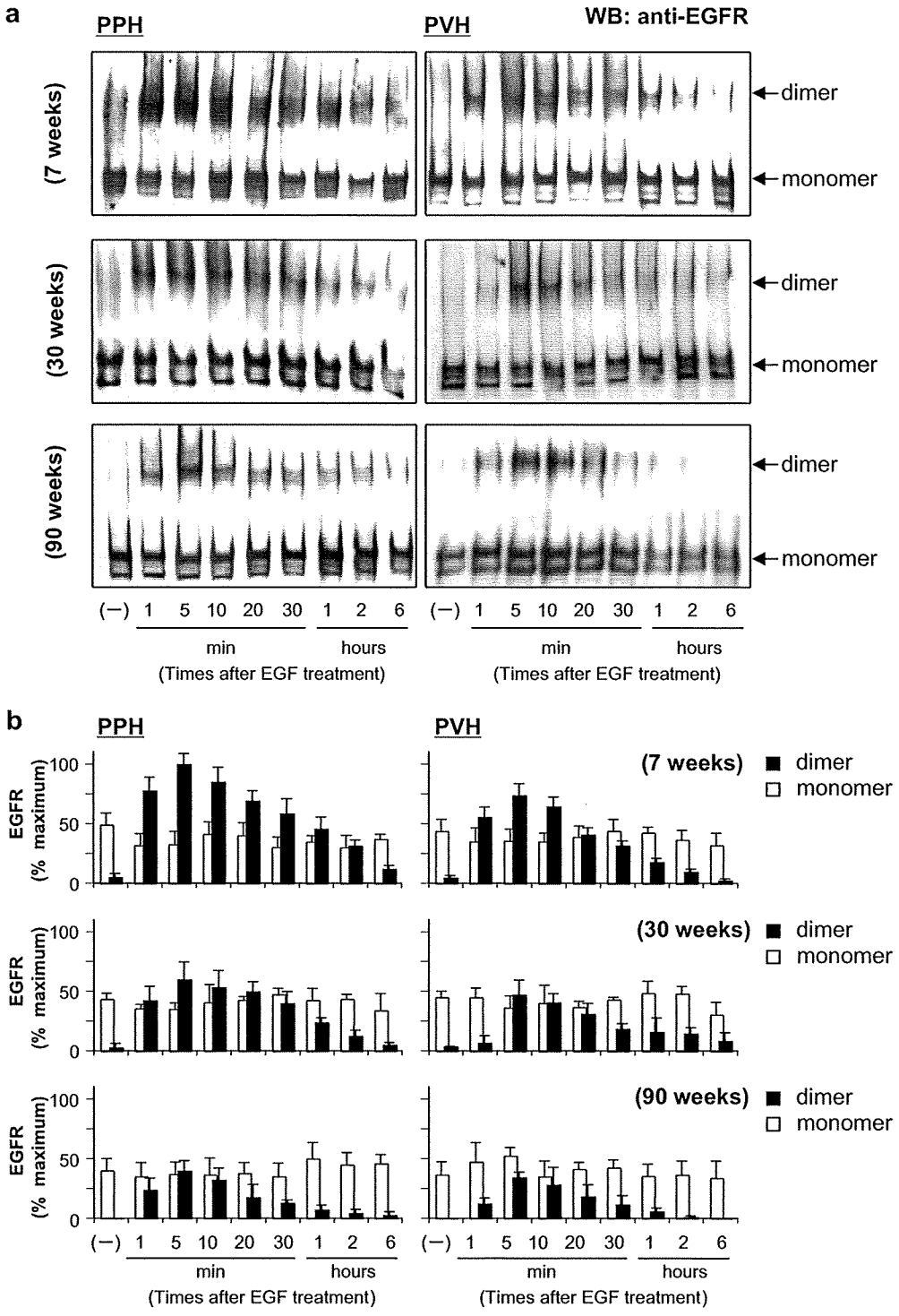

Fig. 3. Effect of aging on EGFR dimerization induced by EGF treatment in primary cultured PPH and PVH obtained from 7-, 30-, and 90-week-old rats. After EGF (10^{-8} M) treatment at intervals: 1 min, 5 min, 10 min, 20 min, 30 min, 1 h, 2 h, and 6 h, the proteins were cross-linked with bis-(sulfosuccinimidyl) suberate (BS^3). The cell membranes obtained from cultured hepatocytes were then lysed and the protein samples were immunoblotted with anti-EGFR antibodies. The band quantitation was performed with National Institutes of Health image software. (a) Immunodetections of EGFRs (monomer and dimer) are shown. Results represent one typical experiment. (b) The histogram represents mean ± SEM of 3 independent experiments, expressed relative to the peak of EGFR dimer in PPH from 7 weeks rats at 5 min following EGF treatment taken as 100%.

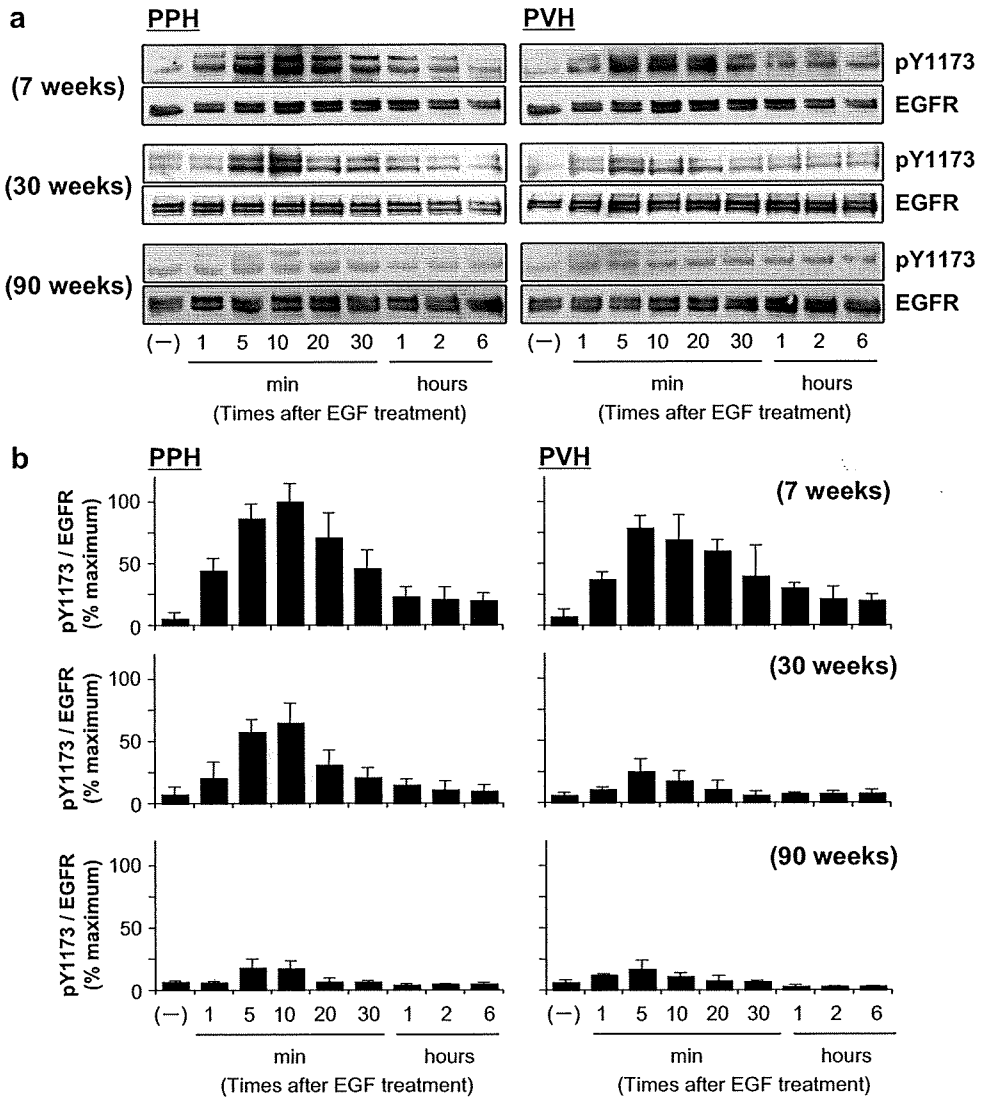

Fig. 4. Effect of aging on EGFR phosphorylation induced by EGF treatment in primary cultured PPH and PVH obtained from 7-, 30-, and 90-week-old rats. After EGF (10^{-8} M) treatment for indicated times, the cell membranes obtained from cultured hepatocytes were lysed and the protein samples were immunoblotted with antibodies to EGFR phosphorylated at Y1173 and EGFR. To determine specific tyrosine phosphorylation of the EGFR, PVDF membranes probed with anti-phosphotyrosine antibody were stripped with a solution of 0.1 M glycine (pH 2.1) and reprobed with anti-EGFR antibody. The band quantitation was performed with National Institutes of Health image software. (a) Immunodetections of EGFR phosphorylation and EGFR are shown. Results represent one typical experiment. (b) The histogram represents mean ± SEM of 3 independent experiments, expressed relative to the peak of the phosphorylation in EGFR in PPH from 7 weeks rats at 10 min following EGF treatment taken as 100%.

teristics including proliferative capacity, EGFR number and ligand affinity.

The binding of EGF to the extracellular domain of its receptor causes dimerization of EGFRs, and its downstream signaling pathways are activated [29,30]. In the present study, EGF-induced dimerization of its receptors was greater in PPH than in PVH obtained from 7-week-old rats; however, this dimerization in both subpopulations reduced with aging (Fig. 3). The present data suggested that this age-related down-regulation of dimerization of EGFRs was related to that of a subclass of high-affinity EGFRs associated with aging. Until now, the relationship between a subclass of high-affinity EGFR and EGFR dimerization was not well understood. But, it is generally assumed that when EGF exists on cell surface, EGF preferentially binds to a subclass of high-affinity receptors, although a subclass of high-affinity EGFRs on liver cell membranes is in equilibrium with the low-affinity state in the absence of EGF [31,32]. Therefore, our data support the hypothesis that the binding of EGF to its receptor in the high-affinity state causes the dimerization of its receptor.

EGF binding induces the dimerization of the receptor, rapidly leading to *trans*-autophosphorylation on the intracellular tyrosine kinase domain and subsequent activation of the downstream signaling pathways [4,32]. Indeed, the present results indicated that the pattern of phosphorylation of EGFR was nearly parallel to that of dimerization of its receptor in cultured PPH and PVH from rats of various ages (Figs. 3 and 4).

Previous studies have demonstrated that EGFRs are unaltered with aging [3,33] and suggested that EGF-induced activation of mitogen-activated protein kinase (MAPK) was reduced, by the elevation in the level of MAPK phosphatase [34]. On the other hand, in aged cells, the EGFR showed reduced ability to interact with the Shc adaptor protein, and this was related to reduced phosphorylation of the EGFR at tyrosine 1173 including the Shc binding domain [22,35]. It has been suggested that the association of Shc to EGFR, leading to its tyrosine phosphorylation and to the recruitment of Grb2, was the main step in EGF-dependent induction of the Ras/MAPK pathway [36]. However, in a different cellular system, Hashimoto et al. have shown that Shc is not necessary for Ras activation by the EGFR [37]. Therefore, in the previous study, the reason for down-regulation of EGF-induced activation of its receptor was unclear. Our present data demonstrate a possibility that age-related decline in EGF-induced DNA synthesis of cultured hepatocytes is caused by down-regulation of EGFR dimerization, which is upstream of its phosphorylation cascade resulting in sequential activation of Ras/MAPK pathway. Moreover, these results were clearly explained by consideration of zonal differences between PPH and PVH, which differed in proliferative capacity. The present data provide valuable information for further studies on age-related decline in DNA synthesis in primary cultured systems.

References

[1] Tsukamoto I, Nakata R, Kojo S. Effect of ageing on rat liver regeneration after partial hepatectomy. Biochem Mol Biol Int 1993;30:773–778.

[2] Wang X, Quail E, Hung NJ, Tan Y, Ye H, Costa RH. Increased levels of forkhead box M1B transcription factor in transgenic mouse hepatocytes prevent age-related proliferation defects in regenerating liver. Proc Natl Acad Sci USA 2001;98:11468–11473.

[3] Ishigami A, Reed TD, Roth GS. Effect of aging on EGF stimulated DNA synthesis and EGF receptor levels in primary cultured rat hepatocytes. Biochem Biophys Res Commun 1993;196:181–186.

[4] Herbst RS. Review of epidermal growth factor receptor biology. Int J Radiat Oncol Biol Phys 2004;59:21–26.

[5] Defize LH, Boonstra J, Meisenhelder J, Kruijer W, Tertoolen LG, Tilly BC, et al. Signal transduction by epidermal growth factor occurs through the subclass of high affinity receptors. J Cell Biol 1989;109:2495–2507.

[6] Bellot F, Moolenaar W, Kris R, Mirakhur B, Verlaan I, Ullrich A, et al. High-affinity epidermal growth factor binding is specifically reduced by a monoclonal antibody, and appears necessary for early responses. J Cell Biol 1990;110:491–502.

[7] Marti U. Handling of epidermal growth factor and number of epidermal growth factor receptors are changed in aged male rats. Hepatology 1993;18:1432–1436.

[8] Jungermann K. Functional heterogeneity of periportal and perivenous hepatocytes. Enzyme 1986;35:161–180.

[9] Gebhardt R. Metabolic zonation of the liver: regulation and implications for liver function. Pharmacol Ther 1992;53:275–354.

[10] Gebhardt R. Different proliferative activity in vitro of periportal and perivenous hepatocytes. Scand J Gastroenterol Suppl 1988;151:8–18.

[11] Ohtake Y, Maruko A, Kojima S, Ono T, Nagashima T, Fukumoto M, et al. Zonal differences in DNA synthesis and in transglutaminase activity between perivenous versus periportal regions of regenerating rat liver. Biol Pharm Bull 2004;27:1758–1762.

[12] Ohtake Y, Suyama S, Abe S, Sato N, Kojima S, Fukumoto M, et al. The involvement of polyamines as substrates of transglutaminase in zonal different hepatocyte proliferation after partial hepatectomy. Biol Pharm Bull 2005;28:349–352.

[13] Maruko A, Ohtake Y, Konno K, Abe S, Ohkubo Y. Transglutaminase differentially regulates growth signalling in rat perivenous and periportal hepatocytes. Cell Prolif 2006;39:183–193.

[14] Gebhardt R, Marti U. Heterogeneous distribution of the epidermal growth factor receptor in rat liver parenchyma. Prog Histochem Cytochem 1992;26:164–168.

[15] Reitman S, Frankel S. A colorimetric method for the determination of serum glutamic oxalacetic and glutamic pyruvic transaminases. Am J Clin Pathol 1957;28:56–63.

[16] Wellner VP, Meister A. Binding of adenosine triphosphate and adenosine diphosphate by glutamine synthetase. Biochemistry 1966;5:872–879.

[17] Lindros KO, Penttila KE. Digitonin-collagenase perfusion for efficient separation of periportal or perivenous hepatocytes. Biochem J 1985;228:757–760.

[18] Gebhardt R. Altered acinar distribution of glutamine synthetase and different growth response of cultured enzyme-positive and -negative hepatocytes after partial hepatectomy. Cancer Res 1990;50:4407–4410.

[19] Hensler PJ, Pereira-Smith OM. Human replicative senescence. A molecular study. Am J Pathol 1995;147:1–8.

[20] Peacocke M, Campisi J. Cellular senescence: a reflection of normal growth control, differentiation, or aging? J Cell Biochem 1991;45:147–155.

[21] Castillo C, Salazar V, Ariznavarreta C, Vara E, Tresguerres JA. Effect of recombinant human growth hormone on age-related hepatocyte changes in old male and female Wistar rats. Endocrine 2004;25:33–39.

[22] Palmer HJ, Tuzon CT, Paulson KE. Age-dependent decline in mitogenic stimulation of hepatocytes. Reduced association between Shc and the epidermal growth factor receptor is coupled to decreased activation of Raf and extracellular signal-regulated kinases. J Biol Chem 1999;274:11424–11430.

[23] Imai K, Mine T, Tagami M, Hanaoka K, Fujita T. Zonal differences in effects of HGF/SF and EGF on DNA synthesis in hepatocytes under fed or starved conditions. Am J Physiol 1998;275:G1394–G1401.

[24] Fukujin H, Fujita T, Mine T. Additivity of the proliferative effects of HGF/SF and EGF on hepatocytes. Biochem Biophys Res Commun 2000;278:698–703.

[25] Nakamura T, Tomita Y, Ichihara A. Density-dependent growth control of adult rat hepatocytes in primary culture. J Biochem (Tokyo) 1983;94:1029–1035.

[26] Nakamura T, Yoshimoto K, Nakayama Y, Tomita Y, Ichihara A. Reciprocal modulation of growth and differentiated functions of

mature rat hepatocytes in primary culture by cell–cell contact and cell membranes. Proc Natl Acad Sci USA 1983;80:7229–7233.
[27] Takehara T, Matsumoto K, Nakamura T. Cell density-dependent regulation of albumin synthesis and DNA synthesis in rat hepatocytes by hepatocyte growth factor. J Biochem (Tokyo) 1992;112:330–334.
[28] Enat R, Jefferson DM, Ruiz-Opazo N, Gatmaitan Z, Leinwand LA, Reid LM. Hepatocyte proliferation in vitro: its dependence on the use of serum-free hormonally defined medium and substrata of extracellular matrix. Proc Natl Acad Sci USA 1984;81:1411–1415.
[29] Lemmon MA, Bu Z, Ladbury JE, Zhou M, Pinchasi D, Lax I, et al. Two EGF molecules contribute additively to stabilization of the EGFR dimer. EMBO J 1997;16:281–294.
[30] Leserer M, Gschwind A, Ullrich A. Epidermal growth factor receptor signal transactivation. IUBMB Life 2000;49:405–409.
[31] Ferguson KM. Active and inactive conformations of the epidermal growth factor receptor. Biochem Soc Trans 2004;32:742–745.
[32] Dawson JP, Berger MB, Lin CC, Schlessinger J, Lemmon MA, Ferguson KM. Epidermal growth factor receptor dimerization and activation require ligand-induced conformational changes in the dimer interface. Mol Cell Biol 2005;25:7734–7742.
[33] Sawada N, Ishikawa T. Reduction of potential for replicative but not unscheduled DNA synthesis in hepatocytes isolated from aged as compared to young rats. Cancer Res 1988;48:1618–1622.
[34] Liu Y, Guyton KZ, Gorospe M, Xu Q, Kokkonen GC, Mock YD, et al. Age-related decline in mitogen-activated protein kinase activity in epidermal growth factor-stimulated rat hepatocytes. J Biol Chem 1996;271:3604–3607.
[35] Hutter D, Yo Y, Chen W, Liu P, Holbrook NJ, Roth GS, et al. Age-related decline in Ras/ERK mitogen-activated protein kinase cascade is linked to a reduced association between Shc and EGF receptor. J Gerontol A Biol Sci Med Sci 2000;55:B125–B134.
[36] Sakaguchi K, Okabayashi Y, Kido Y, Kimura S, Matsumura Y, Inushima K, et al. Shc phosphotyrosine-binding domain dominantly interacts with epidermal growth factor receptors and mediates Ras activation in intact cells. Mol Endocrinol 1998;12:536–543.
[37] Hashimoto A, Kurosaki M, Gotoh N, Shibuya M, Kurosaki T. Shc regulates epidermal growth factor-induced activation of the JNK signaling pathway. J Biol Chem 1999;274:20139–20143.

ELSEVIER

Archives of Medical Research 39 (2008) 560–566

Archives of Medical Research

ORIGINAL ARTICLE

Neutrophil Gelatinase-associated Lipocalin Acts as a Protective Factor against H_2O_2 Toxicity

Mehryar Habibi Roudkenar,[a] Raheleh Halabian,[a] Zahra Ghasemipour,[b] Amaneh Mohammadi Roushandeh,[c] Mahdi Rouhbakhsh,[d] Mahin Nekogoftar,[a] Yoshikazu Kuwahara,[e] Manabu Fukumoto,[d] and Mohammad Ali Shokrgozar[f]

[a]*Research Center, Iranian Blood Transfusion Organization, Tehran Iran*
[b]*Science and Research Center, Department of Biology, Azad University, Tehran, Iran*
[c]*Department of Anatomy, Faculty of Medicine, Medical University of Tabriz, Tabriz, Iran*
[d]*Cellular and Molecular Biology Department, Khatam University, Tehran, Iran*
[e]*Department of Pathology, Institute of Development, Aging and Cancer, Tohoku University, Sendai, Japan*
[f]*National Cell Bank of Iran, Pasteur Institute of Iran, Tehran, Iran*

Received for publication January 26, 2008; accepted May 16, 2008 (ARCMED-D-08-00032).

Background. Lipocalin 2 (Lcn2, NGAL) is a member of the lipocalin superfamily for which a variety of functions have been reported. However, the precise biological roles of NGAL are not fully known. We have investigated the ability of NGAL to prevent H_2O_2 toxicity, which is considered to be the classical inducer of oxidative stress caused by ROS generation in an *in vitro* model.

Methods. NGAL cDNA was isolated from HepG2 cell line and cloned to pcDNA3.1(+) vector. The construct was transfected to CHO cell line. Stable clones were generated, and the expression of NGAL was determined by RT-PCR, Western blot analysis and ELISA. NGAL gene in A549 cell line was downregulated with the siRNA. CHO and A549 cells were intoxicated with H_2O_2 and cell proliferation was performed by MTT assay. Apoptotic cells were detected by flow cytometry.

Results. Cell proliferation was higher in CHO expressing NGAL in doses of 5 and 10 mM H_2O_2 after 2 h compared with the control. H_2O_2 was also more toxic in the presence of NGAL siRNA compared with the control in A549 cell. Our results also revealed that NGAL protect cells from apoptosis.

Conclusions. Overall, our results revealed for the first time a new function for NGAL/Lcn2: acting as a protective factor against H_2O_2 toxicity. In the future, NGAL may have the potential application to ameliorate the toxicity induced by oxidative stress conditions.

Key Words: NGAL/Lcn2, H_2O_2, Toxicity, Protective factor.

Introduction

Lipocalins constitute a broad but evolutionally conserved family of small proteins; however, the functions of many lipocalins remain unclear to date. Neutrophil gelatinase-associated lipocalin (NGAL; also known as lipocalin 2 or human neutrophil lipocalin) is a 25-kDa glycoprotein that was initially purified from neutrophil granules (1). NGAL exists as a 25-kDa monomer, as a 46-kDa homodimer, and in a covalent complex with neutrophil gelatinase, also known as matrix metalloproteinase 9 (2,3). Under various pathophysiological conditions such as infection, cancer, inflammation, kidney injury, cardiovascular disease, burn injury, and intoxication, expression of NGAL is induced (4–13). A variety of functions for NGAL has been reported. These include transport of fatty acid or iron (14,15), induction of apoptosis in cytokine-dependent neutrophils and other leukocytes (16), suppression of bacterial growth

Address reprint requests to: Mehryar Habibi Roudkenar, Research Center, Iranian Blood Transfusion Organization, Tehran, Iran; E-mail: Roudkenar@ibto.ir

0188-4409/08 $–see front matter.
doi: 10.1016/j.arcmed.2008.05.003

(1,17), and modulator of inflammatory responses (2,18). Contrary to previous reports, most functions of Lcn2 except its role in innate immunity are not verified in Lcn2-deficient mice (19). More recently, we found induction of Lcn2/NGAL expression under oxidative stress condition and in β-thalassemia patients (20,21). To clarify the overall functions of NGAL, the present study was designed to determine whether this lipocalin has any protective role against H_2O_2 toxicity. In order to elucidate this hypothesis, NGAL was exogenously expressed in CHO cells that are not apt to such an expression so that the protective effect of NGAL against H_2O_2 treatment would be examined. On the other hand, we also suppressed the NGAL expression by siRNA transfection for the effect of H_2O_2 to be investigated.

Materials and Methods

Cell Culture

HepG2 (human hepatoma cell line), CHO (Chinese hamster ovary cell line) and A549 (lung carcinoma cell line) were obtained from the National Cell Bank of Iran (NCBI). These cell lines were grown in RPMI-1640 medium (Gibco-BRL, Eggenstein, Germany) with 10% fetal bovine serum (Gibco-BRL).

Expression of NGAL in Cell Culture

Total RNA was extracted by Trizol reagent (Invitrogen, Carlsbad, CA) according to the manufacturer's protocol. RNA quality was determined by electrophoresis. Reverse transcription was performed by SuperScript III reverse transcriptase (Invitrogen) with 500 ng of total RNA followed by DNaseI (Invitrogen) treatment and heat inactivation. Using RT-PCR, full-length human NGAL was isolated. Expression of NGAL in CHO cells was also examined. PCR was performed using Pfu polymerase (Cinnagene, Tehran, Iran) in a GeneAmp PCR system 9600 (PerkinElmer Life and Analytical Sciences, Wellesley, MA). After initial denaturation (5 min at 94°C), cDNA was subjected to 30 cycles of PCR. Primer set for full-length human *NGAL* containing Kozak sequence, *ECO*RI (forward), and *NOT*I (reverse) restriction enzyme site was forward: 5′-ACG AAT TCA CCA TGG TGC CCC TAG GTC TCC TGT GGC TG-3′; reverse: 5′-TAG CGG CCG CTC AGC CGT CGA TAC ACT GGT C-3′.

Primer set for 240-bp fragments of NGAL was forward: 5′-TCA CCT CCG TCC TGT TTA GG-3′; reverse: 5′-CGA AGT CAG CTC CTT GGT TC-3′. For normalization, expression of β-actin was examined; forward: 5′-TTC TAC AAT GAG CTG CGT GTG G -3′; reverse: 5′-GTG TTG AAG GTC TCA AAC ATG AT-3′.

PCR annealing temperature was 60°C for human *NGAL* and 59°C for β-actin. PCR products were separated in 2% agarose gel. Using real-time PCR, reduction of NGAL gene expression after siRNA administration was examined with a BIO-RAD icycler iQ, SA-THK Real-Time PCR system (Bio-Rad Laboratories, Hercules, CA). Amplification was conducted using AB solute syber green ROX mix (ABgene) according to the manufacturer's instruction. PCR condition was initial denaturation at 94°C for 15 min. followed by 40 amplification cycles consisting of denaturation at 94°C for 30 sec, annealation at suitable temperature for 30 sec and extension at 72°C for 30 sec. Threshold cycle values were normalized by β-actin expression.

Establishment of Human NGAL-expressing Cells

To construct the NGAL expression plasmid, the full-length human NGAL cDNA was synthesized by RT-PCR. The amplified NGAL cDNA containing *ECO*RI and *NOT*I restriction enzyme sites was cloned into the mammalian expression vector pcDNA3.1(+) (Invitrogen) in the sense orientation. The identity and orientation of this construct were confirmed by DNA sequencing. CHO cells were transfected with 1 μg of linearized pcDNA3.1−NGAL using the fugene 6 (Roche, Mannheim, Germany) according to the manufacturer's protocol. pcDNA3.1 (+) DNA was used as a control. CHO cells stably expressing human NGAL were selected in a medium containing 600 μg/mL Geneticin (Roche) for at least 14 days leading several stable clones. The expression level of NGAL was examined by RT-PCR, ELISA (R&D Systems, Minneapolis, MN) and western blot analysis using Lcn2 antibody (Santa Cruz Biotechnology, Santa Cruz, CA) with 0.7 μg/mL peroxidase conjugated rabbit anti-mouse IgG (Dako, Glostrup, Denmark) as the secondary antibody.

Small Interfering RNA (siRNA) Gene Silencing

NGAL mRNA was downregulated with Hs_Lcn2_6_HP validated siRNA (Qiagen, Hilden, Germany). Sequences of control siRNA (Qiagen) were sense: UUC UCC GAA CGU GUC ACG U dT dT and antisense: ACG UGA CAC GUU CGG AGA A dT dT.

Five nM of the synthetic double-stranded siRNA oligonucleotides was then delivered into A549 cells using different doses of HiPerFect transfection reagent (Qiagen) according to the manufacturer's protocol. Silencing of NGAL gene expression was measured both by real-time PCR 72 h post-transfection and by the assessment of the amount of NGAL protein simultaneously secreted into the medium.

Cytotoxicity Assays

The cytotoxic effect of H_2O_2 administration was determined by trypan blue dye exclusion and MTT assays. For MTT assay, 2×10^4 cells were seeded/well in a 96-well plate. After 24 h, different concentrations of H_2O_2 (Sigma, Dusseldorf, Germany) were added to each well. At the

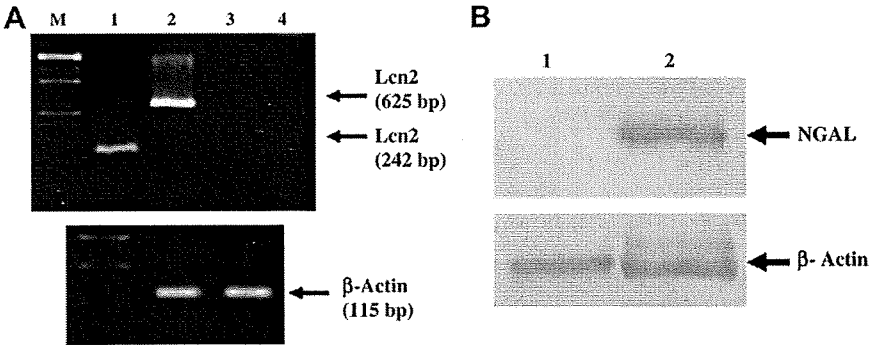

Figure 1. (A) Expression of NGAL in stables clones of CHO. RNA was extracted from CHO cells transfected with the pcDNA3.1-NGAL and CHO cells transfected with the pcDNA3.1. cDNA was synthesized and RT-PCR was performed using two pairs of primers specific for Lcn2. CHO cells transfected with the construct expressed NGAL mRNA, a 240-bp fragment (Lane 1) and full length of NGAL mRNA, 625 (Lane 2), whereas in CHO cells transfected with pcDNA3.1 no expression was observed (Lanes 3 and 4). Lower figure indicating the expression of β-actin in both stable clones of CHO, i.e., transfected with the pcDNA3.1-NGAL and pcDNA3.1 vector. M; 100-bp ladder marker. (B) Western blot analysis of NGAL expression in the stables clones. CHO cells transfected with the construct expressed NGAL protein (Lane 2), whereas in CHO cells transfected with pcDNA3.1 no expression was observed (Lane 2). Color version of this figure available online at www.arcmedres.com

appropriate time point, cells were incubated with 10 μL of 3-(4,5-dimethlthiazol-2-yl)-2,5-diphenyltetrazolium bromide (MTT, Sigma) with concentration of 5 mg/mL at 37°C in 5% CO_2 atmosphere for 4 h. Reaction was stopped by addition of 10% SDS, 0.01 M HCl, and cell viability was measured using a plate reader. We also examined the number of viable cells by trypan blue exclusion assay.

Detection of Apoptosis and Necrosis

Apoptotic and necrotic cells were quantified by flow cytometry after double staining of cells with annexin-V-green fluorescent protein (GFP) and propidium iodide (PI) using Annexin-V-FLOUS staining kit in accordance with the manufacturer's protocol (Roche). Briefly, appropriate cells were incubated at different concentration levels of H_2O_2 and different interval times. Afterwards, cells were detached with trypsin (0.25%) and EDTA (0.5 mM). Detached cells were combined with the floating cells of each well. After incubation with annexin-V-GFP and PI, cells were analyzed by flow cytometry. Annexin-V-positive and PI-positive cells were considered to be apoptotic and necrotic cells, respectively.

Statistical Analysis

Results are expressed as mean ± SD of three independent experiments. Differences were compared using ANOVA with Tukey-Kramer Multiple Comparison Test.

Results

Expression of NGAL in CHO Cell Line

To investigate whether NGAL transfected cells express human NGAL, RT-PCR was performed. Stable clones were isolated after transfection expressed NGAL mRNA, but there was no expression in the CHO cell transfected with pcDNA3.1 (Figure 1A). The cell culture medium of stably human NCAL transfected cells was used for detection of NGAL protein by ELISA and Western blot analysis. Cells transfected with pcDNA3.1-NGAL express NGAL protein, whereas cells transfected with pcDNA3.1 vector do not (Table 1 and Figure 1B). Several stable clones expressing human NGAL were established and one that expressed high yield, 0.25 μg/mL of recombinant NGAL was used for cytotoxicity and apoptosis assay to be conducted after treatment with H_2O_2.

NGAL-expressing CHO Cells Decreased H_2O_2 Toxicity

To test the involvement of NGAL in cell survival after treatment with H_2O_2, stable CHO cells expressing NGAL and a control transfected clone were treated with different doses of H_2O_2 at different time intervals; cytotoxicity and proliferation assays followed. Cell proliferation was higher in CHO cells expressing NGAL in doses of 5 and 10 mM H_2O_2 after 2 h compared to the control (Figure 2) suggesting NGAL role as a protective factor against H_2O_2. The significance level of difference between control CHO and CHO cells expressing NGAL at the first data points (no H_2O_2 exposure) was 0.086.

Table 1. ELISA for human NGAL immunoassay

Samples	OD 450
Lcn2[a] (10 ng/mL)	1.752 ± 0.123
Lcn2[a] (5 ng/mL)	0.912 ± 0.165
Lcn2[a] (2.5 ng/mL)	0.533 ± 0.116
Lcn2[a] (1.25 ng/mL)	0.294 ± 0.094
CHO–pcDNA3.1/Lcn2[b]	1.85 ± 0.162
CHO–pcDNA3.1	0.095 ± 0.032

[a]Standard concentrations of human Lcn2 provided in the ELISA kit.
[b]25-fold dilution.

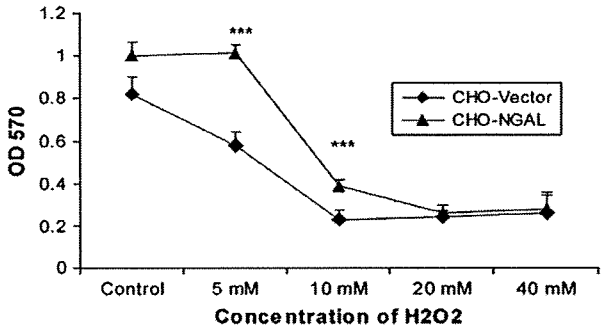

Figure 2. Cytotoxicity effects of different concentrations of H_2O_2 on stable CHO cells transfected with pcDNA3.1-NGAL or pcDNA3.1 for 2 h in MTT assay. Cell proliferation in CHO transfected with construct was higher than control at concentration of 5 and 10 mM H_2O_2, whereas CHO cells transfected with pcDNA3.1 susceptible at these concentration. (Mean ± SD; ***p <0.001; number of replicates, 4). Color version of this figure available online at www.arcmedres.com

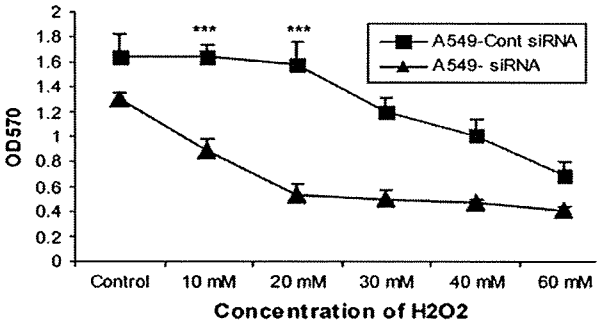

Figure 4. Cytotoxicity effects of different concentration of H_2O_2 on A549 downregulated NGAL (siRNA+) and control siRNA for 2.5 h in MTT assay. Cell proliferation in downregulated NGAL (siRNA+) A549 cells were less than control at concentration of 10 and 20 mM H_2O_2 compared to control. (Mean ± SD; ***p <0.001; number of replicates, 4). Color version of this figure available online at www.arcmedres.com

Downregulation of NGAL Increasing Sensitivity to H_2O_2 Toxicity

In order to analyze the effect of NGAL gene silencing, siRNA was transfected. A549 cells in which NGAL expression was downregulated with siRNA (Figures 3A and 3B) and those transfected with control siRNA were treated with different doses of H_2O_2. H_2O_2 at concentrations of 10 and 20 mM was more toxic in the presence of NGAL siRNA compared with the control (Figure 4). The significance level of the difference between control A549 and A549 cells downregulated with siRNA at the first data points (no H_2O_2 exposure) was 0.002.

Role of NGAL in Cell Protection against Apoptosis

We next examined the role of NGAL in the induction of apoptosis. CHO cells expressing NGAL and A549 cells in which NGAL was downregulated by siRNA were treated with H_2O_2 and apoptosis was assessed by flow cytometry. Twenty four hours after administration of 100 and 200 μM H_2O_2, the number of apoptotic CHO cells expressing NGAL was lower than empty vector transfected cells (Figure 5A and 5C). Seven hours after administration of 80 μM H_2O_2, the number of apoptotic cells in the A549 HGAL downregulated cells was higher than control siRNA transfected cells, indicating the role of NGAL in protecting cells from oxidative stress-induced apoptosis (Figures 5B and 5C).

Discussion

The precise biological roles of Lcn2 are not yet fully known yet. We recently found that ROS can induce NGAL/Lcn2 expression (20). Oxidative stress has been implicated in several harmful conditions such as Alzheimer's disease, cardiovascular disease, transplantation, burn injury, inflammation,

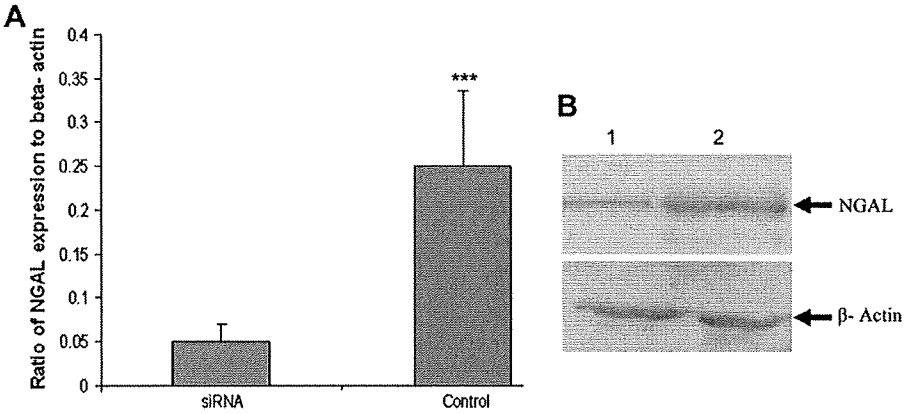

Figure 3. Downregulation of NGAL expression in A549 cell lines were measured by real-time PCR and also by the assessment of the amount of NGAL protein secreted into the medium by Western blot analysis. (A) Real-time RT- PCR. (Mean ± SD; ***p <0.001; number of replicates; 4. (B) Western blot analysis. Lane 1, A549 cell line transfected with siRNA and Lane 2 A549 cell line transfected with control siRNA. Expression of NGAL in A549 cells transfected with siRNA was downregulated in A549 cell transfected with siRNA compared with the control. Color version of this figure available online at www.arcmedres.com

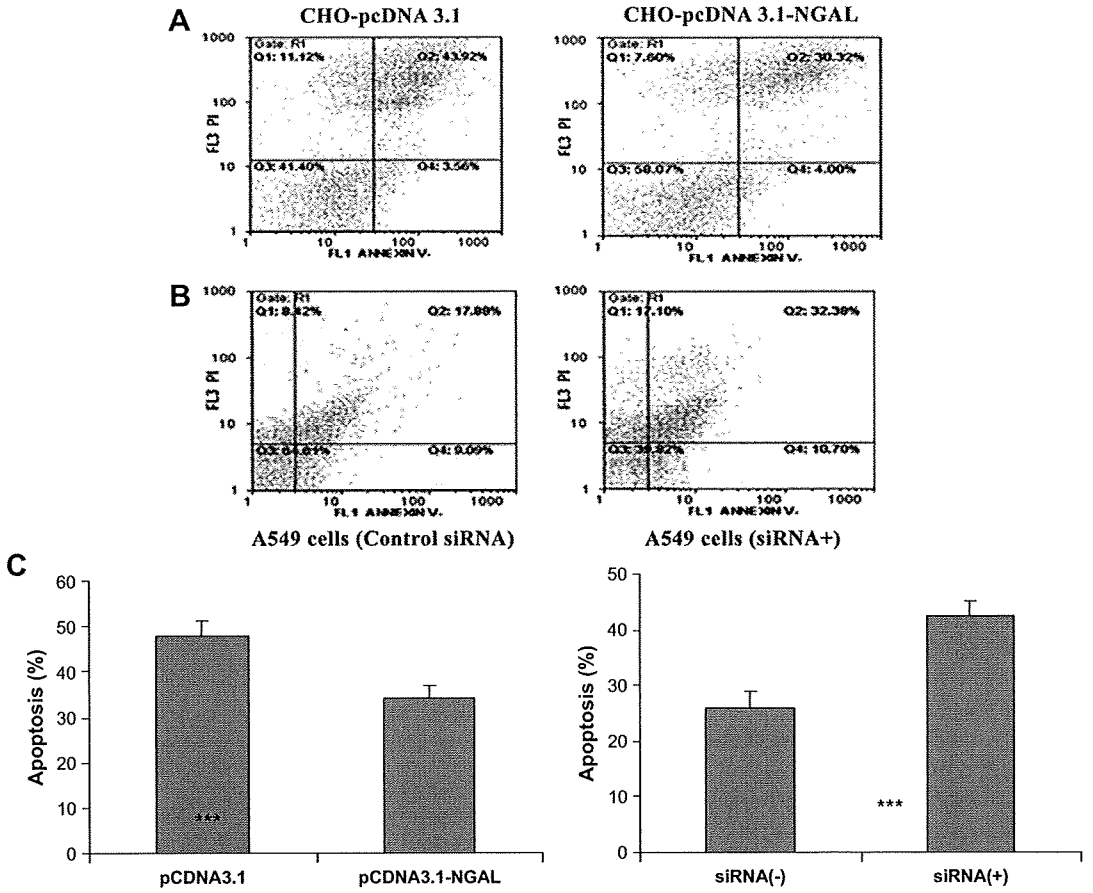

Figure 5. (A) Apoptotic effects of 200 μM H_2O_2 on stable CHO cells transfected with pcDNA3.1-NGAL or pcDNA3.1 for 24 h in flow cytometry. CHO cells transfected with construct presented less apoptotic cells compared with CHO cells transfected with empty vector. (B) Apoptotic effects of 80 μM H_2O_2 on A549 downregulated NGAL (siRNA+) cells and A549 control siRNA for 7 h in flow cytometry. A549 downregulated NGAL presented higher apoptotic cells compared with control siRNA. (C) Apoptosis percent (mean ± SD; ***p <0.001; number of replicates, 3). Color version of this figure available online at www.arcmedres.com

diabetes, and aging (22–27). In this study, we sought to determine the role of NGAL under oxidative stress conditions; in other words, the current study was designed to determine whether NGAL could act as a cytoprotective factor against H_2O_2 toxicity, which is considered to be the classical inducer of oxidative stress caused by ROS generation in an *in vitro* model. The recombinant pcDNA 3.1–NGAL was constructed and transfected to CHO cells. This cell line does not express human NGAL; therefore, after ectopical expression of NGAL any change in cell viability after treatment with H_2O_2 would be due to the recombinant NGAL. We further tested our hypothesis by downregulation of NGAL expression in A549 cells by gene-silencing technology. Our results revealed that NGAL acts as a cytoprotective factor against H_2O_2 toxicity.

A variety of functions has been reported for NGAL. For example, elevated Lcn2 expression in certain human neoplastic diseases (5,6,28) and its association with MMP-9 (29) suggest a role in tumor progression. Upregulated Lcn2 expression in the colon epithelium is associated with a variety of inflammatory conditions (18) and its induction by IL-1β in A549 cells (30) demonstrates an involvement in immunomodulation. Despite the fact that there is little similarity between Lcn1 (another member of the lipocalin family) and Lcn2, they commonly exhibit antimicrobial activity (1,17,31). Lcn1 acts as an oxidative stress-induced scavenger of potentially harmful lipid peroxidation products in a cell culture system (32). It also has been shown that oxidative stress can induce both genes (20,32). Therefore, it seems that both genes have similar function. More recently, Akerstrom et al. showed that α1-micogolobulin, another member of the lipocalin family, acts as scavenger for free radicals (33). Lipocalin 2 has been strongly implicated as a pro-apoptotic factor. However, our results revealed that NGAL protects cell from apoptosis. Thorsten et al., using Lcn2-deficient mice, showed that lipocalin 2 is not essential for apoptosis induced by IL-3 withdrawal (19). Tong et al. showed that downregulation of NGAL expression by siRNAs decreases further the inhibition of proliferation induced by a PDK1 inhibitor, whereas overexpression of

NGAL reduces cell death (necrosis and apoptosis) induced by this compound, supporting our results (34). They also proved that purified NGAL protein had no cytotoxic effects, whereas an antiserum against full-length NGAL was toxic. Therefore, induction of NGAL with different apoptotic stimuli could be due to compensatory response.

In our study, cell proliferation in CHO-NGAL cell line was higher compared to CHO-vector. On the contrary, in downregulated A549 (treated with siRNA) it was lower compared to control A549 cell line suggesting NGAL as a surviving or cytoprotective factor essential for normal physiology of the cells. One of the reasons for the above results may be attributed to the scavenging role of NGAL against ROS physiologically produced in culture medium.

There was a significant difference between control A549 and A549 cells downregulated with siRNA at the first data points (no H_2O_2 exposure). This may argue against our hypothesis that NGAL is protective against H_2O_2. However, the difference between control A549 and A549 cells downregulated with siRNA at the concentrations of 10 and 20 mM of H_2O_2 was much more significant compared with that of the first data points (no H_2O_2 exposure); this indicates that some of the effects may be due to an independent survival-promoting effect of NGAL.

NGAL has been identified as an iron-transporting protein (35). It is well known that the delivery of iron to cells is crucial for cell growth and development. Therefore, the functions of NGAL in the support of cell survival may occur through the transport of iron, retinal or other molecules that make cells more resistant to toxic stress. Additional support for the survival activity of NGAL comes from Sorensen et al. (36), who reported that NGAL was strongly induced by growth factors including IGF and TGF-α in primary human keratinocytes. This induction is believed to play a role in wound healing. Furthermore, NGAL can protect against acute ischemic renal injury (37) and downregulation of *ExFABP*, a related chicken lipocalin, by transient transfection with antisense *ExFABP* induces apoptosis in chicken embryo chondrocytes (38). More recently, we reported the upregulation of NGAL in β-thalassemia patients (21). In this study, we report the protective role of NGAL against ROS. Together this indicates the beneficial role of NGAL induction in β-thalassemia patients.

In summary, in this study we explored a new function for NGAL, a cell protective factor against H_2O_2 toxicity. In the future, NGAL may have the potential application to ameliorate the toxicity induced by oxidative stress conditions such as Alzheimer's disease, thalassemia, cardiovascular disease, burn injury, transplantation, diabetes, and aging.

References

1. Flower DR, North AC, Sansom CE. The lipocalin protein family: structural and sequence overview. Biochim Biophys Acta 2000;1482:9–24.
2. Bundgaard JR, Sengelov H, Borregaard N, Kjeldsen L. Molecular cloning and expression of a cDNA encoding Ngal: a lipocalin expressed in human neutrophils. Biochem Biophys Res Commun 1994;202:1468–1475.
3. Cowland JB, Borregaard N. Molecular characterization and pattern of tissue expression of the gene for neutrophil gelatinase-associated lipocalin from humans. Genomics 1997;45:17–23.
4. Flo TH, Smith KD, Sato S, Rodriguez DJ, Holmes MA, Strong RK, et al. Lipocalin 2 mediates an innate immune response to bacterial infection by sequestrating iron. Nature 2004;432:917–921.
5. Missiaglia E, Blaveri E, Terris B, Wang YH, Costello E, Neoptolemos JP, et al. Analysis of gene expression in cancer cell lines identifies candidate markers for pancreatic tumorigenesis and metastasis. Int J Cancer 2004;112:100–112.
6. Santin AD, Zhan F, Bellone S, Palmieri M, Cane S, Bignotti E, et al. Gene expression profiles in primary ovarian serous papillary tumors and normal ovarian epithelium: identification of candidate molecular markers for ovarian cancer diagnosis and therapy. Int J Cancer 2004;112:14–25.
7. Liu Q, Nilsen-Hamilton M. Identification of a new acute phase protein. J Biol Chem 1995;270:22565–22570.
8. Mishra J, Mori K, Ma Q, Kelly C, Barasch J, Devarajan P. Neutrophil gelatinase-associated lipocalin: a novel early urinary biomarker for cisplatin nephrotoxicity. Am J Nephrol 2004;24:307–315.
9. Hemdahl AL, Gabrielsen A, Zhu C, Eriksson P, Hedin U, Kastrup J, et al. Expression of neutrophil gelatinase-associated lipocalin in atherosclerosis and myocardial infarction. Arterioscler Thromb Vasc Biol 2006;26:136–142.
10. Mishra J, Ma Q, Prada A, Mitsnefes M, Zahedi K, Yang J, et al. Identification of neutrophil gelatinase-associated lipocalin as a novel early urinary biomarker for ischemic renal injury. J Am Soc Nephrol 2003; 14:2534–2543.
11. Mishra J, Dent C, Tarabishi R, Mitsnefes MM, Ma Q, Kelly C, et al. Neutrophil gelatinase-associated lipocalin (NGAL) as a biomarker for acute renal injury after cardiac surgery. Lancet 2005;365: 1231–1238.
12. Vemula M, Berthiaume F, Jayaraman A, Yarmush ML. Expression profiling analysis of the metabolic and inflammatory changes following burn injury in rats. Physiol Genomics 2004;18:87–98.
13. Kirstin M, Ju-Seog L, Patricia AD, Wen-Qing CM, Sambasiva R, Snorri ST, et al. Molecular profiling of hepatocellular carcinomas developing spontaneously in acyl-CoA oxidase deficient mice: comparison with liver tumors induced in wild-type mice by a peroxisome proliferator and a genotoxic carcinogen. Carcinogenesis 2003;24: 975–984.
14. Triebel S, Blaser J, Reinke H, Tschesche H. A 25 kDa α2-microglobulin-related protein is a component of the 125 kDa form of human gelatinase. FEBS Lett 1992;314:386–388.
15. Chu ST, Lin HJ, Huang HL, Chen YH. The hydrophobic pocket of 24p3 protein from mouse uterine luminal fluid: fatty acid and retinol binding activity and predicted structural similarity to lipocalins. J Pept Res 1998;52:390–397.
16. Devireddy LR, Teodoro JG, Richard FA, Green MR. Induction of apoptosis by a secreted lipocalin that is transcriptionally regulated by IL-3 deprivation. Science 2001;293:829–834.
17. Goetz DH, Holmes MA, Borregaard N, Bluhm ME, Raymond KN, Strong RK. The neutrophil lipocalin NGAL is a bacteriostatic agent that interferes with siderophore-mediated iron acquisition. Mol Cell 2002;10:1033–1043.
18. Nielsen BS, Borregaard N, Bundgaard JR, Timshel S, Sehested M, Kjeldsen L. Induction of NGAL synthesis in epithelial cells of human colorectal neoplasia and inflammatory bowel disease. Gut 1996;38: 414–420.
19. Thorsten B, Atsushi T, Gordon SD, Andrew JE, Annick YT, Andrew W, et al. Lipocalin 2-deficient mice exhibit increased sensitivity to

Escherichia coli infection but not to ischemia-reperfusion injury. Proc Natl Acad Sci USA 2006;7:1834–1839.
20. Roudkenar MH, Kuwahara Y, Baba T, Roushandeh AM, Ebishima SH, Abe SH, et al. Oxidative stress induced Lipocalin 2 gene expression, addressing its expression under the harmful condition. J Radiat Res 2007;48:39–44.
21. Roudkenar MH, Halabian R, Oodi A, Yaghmai P, Roushandeh AM, Najar MR, et al. Upregulation of neutrophil gelatinase-associated lipocalin, NGAL/Lcn2, in β thalassemia patients. Arch Med Res 2008; 39:402–407.
22. Loh KP, Huang SH, De Silva R, Tan BK, Zhu YZ. Oxidative stress: apoptosis in neuronal injury. Curr Alzheimer Res 2006;3:327–337.
23. Frank JG. Oxygen, oxidative stress, hypoxia, and heart failure. J Clin Invest 2005;115:500–508.
24. Zhang W, Wang M, Xie HY, Zhou L, Meng XQ, Shi J, et al. Role of reactive oxygen species in mediating hepatic ischemia-reperfusion injury and its therapeutic applications in liver transplantation. Transplant Proc 2007;39:1332–1337.
25. Dröge W, Schipper HM. Oxidative stress and aberrant signaling in aging and cognitive decline. Aging Cell 2007;63:361–370.
26. Jureta WH. Free radicals and lipid peroxidation mediated injury in burn trauma: the role of antioxidant therapy. Toxicology 2003;189: 75–88.
27. Martínez JA. Mitochondrial oxidative stress and inflammation: an slalom to obesity and insulin resistance. J Physiol Biochem 2006;62: 303–306.
28. Stoesz SP, Friedl A, Haag JD, Lindstrom MJ, Clark GM, Gould MN. Heterogeneous expression of the lipocalin NGAL in primary breast cancers. Int J Cancer 1998;79:565–572.
29. Yan L, Borregaard N, Kjeldsen L, Moses MA. The high molecular weight urinary matrix metalloproteinase (MMP) activity is a complex of gelatinase B/MMP-9 and neutrophil gelatinase-associated lipocalin (NGAL). Modulation of MMP-9 activity by NGAL. J Biol Chem 2001;276:37258–37265.
30. Cowland JB, Sorensen OE, Sehested M, Borregaard N. Neutrophil gelatinase-associated lipocalin is up-regulated in human epithelial cells by IL-1 beta, but not by TNF-α. J Immunol 2003;171:6630–6639.
31. Maria F, Hubertus H, Petra M, Ben JG, Bernhard R. Human tear lipocalin exhibits antimicrobial activity by scavenging microbial siderophores. Antimicrob Agents Chemother 2004;48:3367–3372.
32. Markus L, Petra W, Bernhard R. Human tear lipocalin acts as an oxidative-stressinduced scavenger of potentially harmful lipid peroxidation products in a cell culture system. Biochem J 2001;356:129–135.
33. Åkerström B, Maghzal G, Winterbourn C, Kettle AJ. The lipocalin α1-microglobulin has radical scavenging activity. JBC 2007;282: 31493–31503.
34. Tong Z, Wu X, Ovcharenko D, Zhu J, Chen CS, Kehrer JP. Neutrophil gelatinase-associated lipocalin as a survival factor. Biochem J 2005; 391:441–448.
35. Yang J, Goetz D, Li JY, Wang W, Mori K, Setlik D, et al. An iron delivery pathway mediated by a lipocalin. Mol Cell 2002;10: 1045–1056.
36. Sorensen OE, Cowland JB, Theilgaard-Monch K, Liu L, Ganz T, Borregaard N. Wound healing and expression of antimicrobial peptides/ polypeptides in human keratinocytes, a consequence of common growth factors. J Immunol 2003;170:5583–5589.
37. Mishra J, Mori K, Ma Q, Kelly C, Jang J, Mitsnefes M, et al. Amelioration of ischemic acute renal injury by neutrophil gelatinase-associated lipocalin. J Am Soc Nephrol 2004;15:3073–3082.
38. Di Marco E, Sessarego N, Zerega B, Cancedda R, Cancedda FD. Inhibition of cell proliferation and induction of apoptosis by ExFABP gene targeting.